ORIENTATION CHARACTERISTICS OF THE MICROSTRUCTURE OF MATERIALS.

Crystallographic orientations, Misorientations, Image Quality Factors.

K. Sztwiertnia

Polish Academy of Sciences, Institute of Metallurgy and Materials Science, 25 Reymonta St., 30-059 Krakow, Poland

K. Sztwiertnia: *Orientacja krystalograficzna w badaniach mikrostruktury materiałów*, Polska Akademia Nauk, Instytut Metalurgii i Inżynierii materiałowej, ISBN 978-83-607 68 02 0, Kraków 2009, 1-98.

Contents

Introduction to SEM and TEM-base orientation imaging microscopy (OIM) techniques.

●Quantitative microstructure image in the **nano scale** (Transmission Electron Microscope TEM).

Example I: Investigation of recrystallization processes.
Example II: OIM applied to gradient materials.

● Quantitative microstructure image in the **micro scale** (Scanning Electron Microscope SEM).

Example III: OIM applied to composites.
Example IV: Image Quality Maps.

OIM or COM; what is it?

OIM® = Orientation Imaging Microscopy®

COM = Crystal Orientation Mapping

COM=OIM

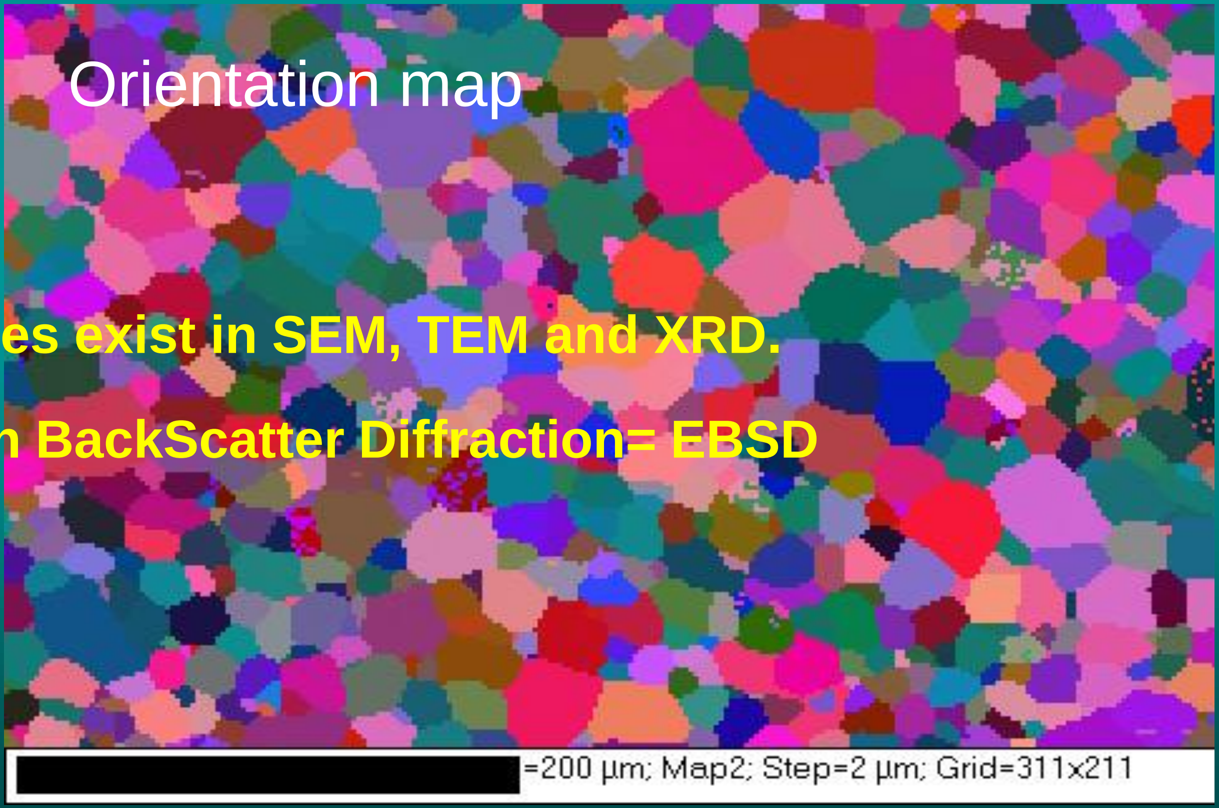

Techniques exist in SEM, TEM and XRD.

Electron BackScatter Diffraction= EBSD

Crystallographic orientation

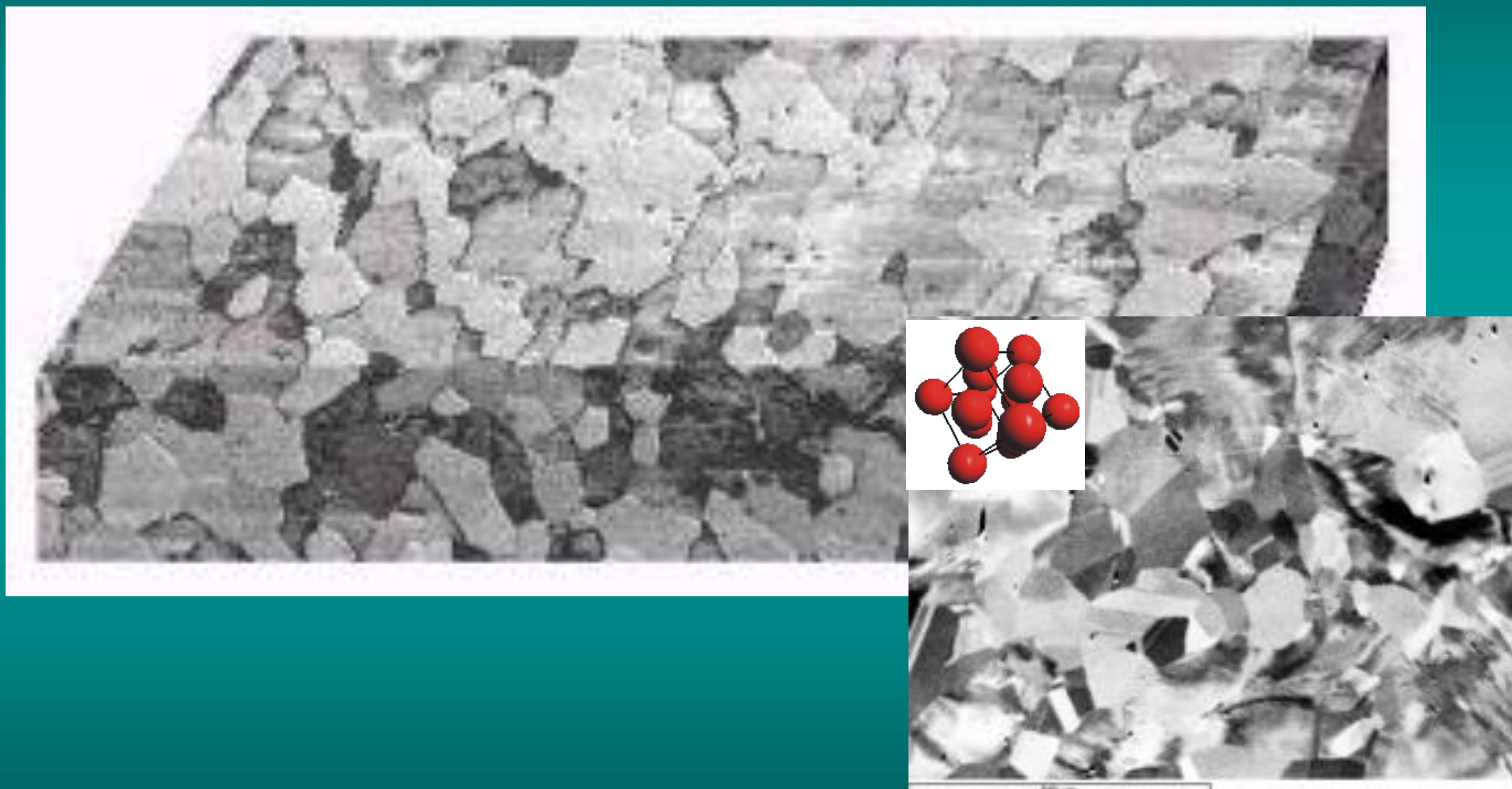

Polycrystalline material → an aggregate of single crystal grains.

K. Sztwiertnia

Crystallographic orientation

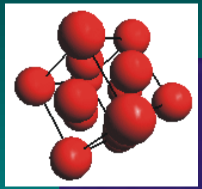

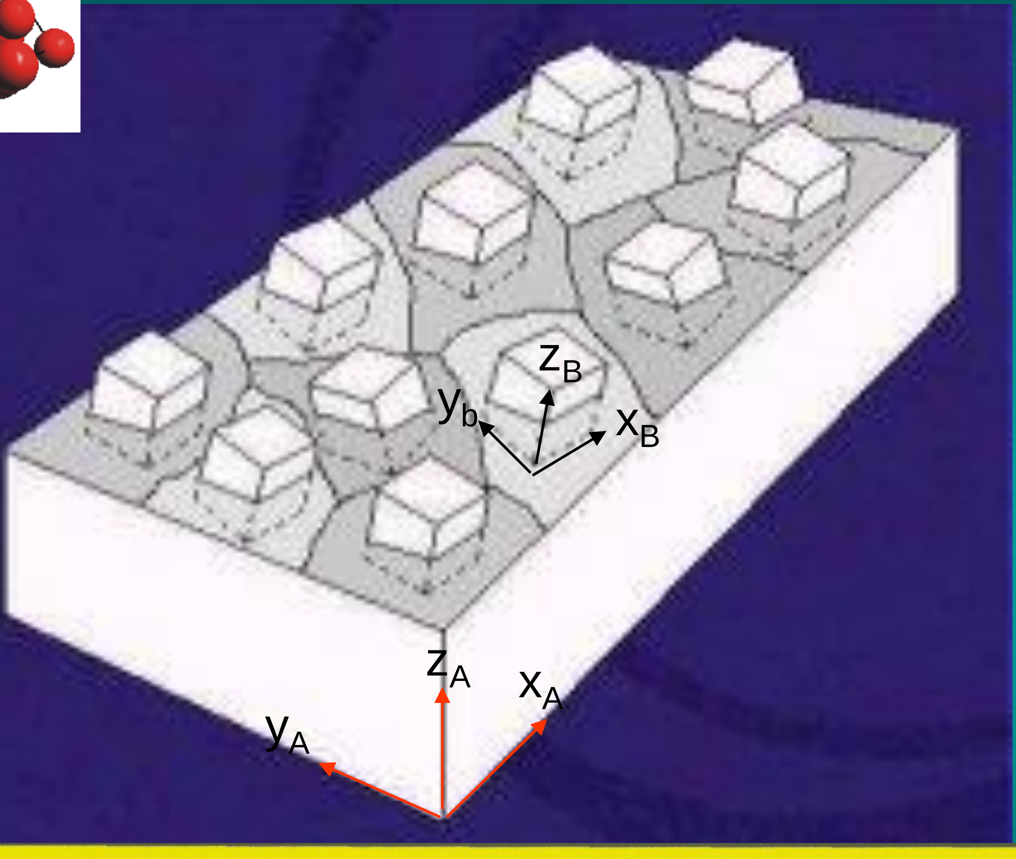

The orientation ☞ a rotation or a set of special rotations with the help of them a coordinate system K_A will be oriented parallel to K_B (K_A and K_B ☞ right-handed rectangular systems).

The orientation ☞ unambiguously characterised by three numbers combined in the symbol g.

$$K_B = g \cdot K_A$$

Crystallographic orientation

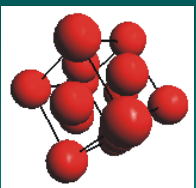

If the crystal lattice possesses rotation symmetries ☞ there are $N_B>1$ equivalent, physically undistinguishable K_{Bj} coordinate systems.

$$K_{B_j} = g_{B_j} \cdot K_B$$

In addition to the crystal symmetry, there can also be symmetries in the sample fixed coordinate system.

$$K_{A_i} = g_{A_i} \cdot K_A$$

$$\boxed{K_{B_{ji}} = g_{B_j} \cdot g \cdot g_{A_i} \cdot K_A}$$

Crystallographic orientation

$$g = \begin{bmatrix} a_{11} & a_{12} & a_{13} \\ a_{21} & a_{22} & a_{23} \\ a_{31} & a_{32} & a_{33} \end{bmatrix}$$

The direction cosines a_{ij} of the angle between the i-th axis of the B system, and the j-th axis of A system are the natural parameters which characterize the orientation of one system against another one.

The matrix g containing the direction cosines a_{ij} is called orientation matrix.

Crystallographic orientation

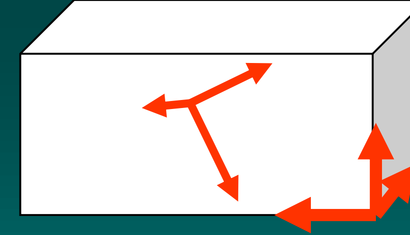

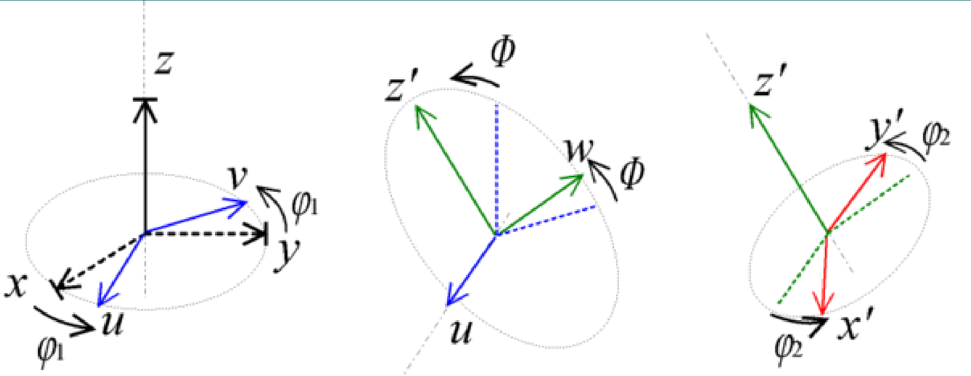

Bunge

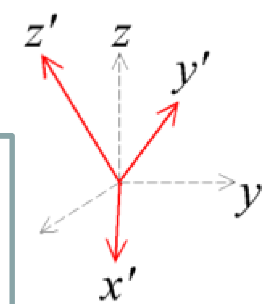

$$g = \begin{bmatrix} \cos\varphi_1\cos\varphi_2 - \sin\varphi_1\sin\varphi_2\cos\phi & \sin\varphi_1\cos\varphi_2 + \cos\varphi_1\sin\varphi_2\cos\phi & \sin\varphi_2\sin\phi \\ -\cos\varphi_1\sin\varphi_2 - \sin\varphi_1\cos\varphi_2\cos\phi & -\sin\varphi_1\sin\varphi_2 + \cos\varphi_1\cos\varphi_2\cos\phi & \cos\varphi_2\sin\phi \\ \sin\varphi_1\sin\phi & -\cos\varphi_1\sin\phi & \cos\phi \end{bmatrix}$$

Example of two different ways to define the orientation. The first way is the only one used in solid mechanics, the angles are noted (ψ,θ,φ). In materials sciences, Bunge, who is one of the reference in crystallite orientation, uses different names: $(\varphi_1,\Phi,\varphi_2)$.

K. Sztwiertnia

Crystallographic orientation

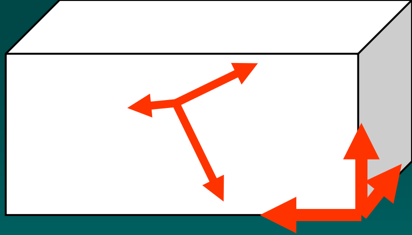

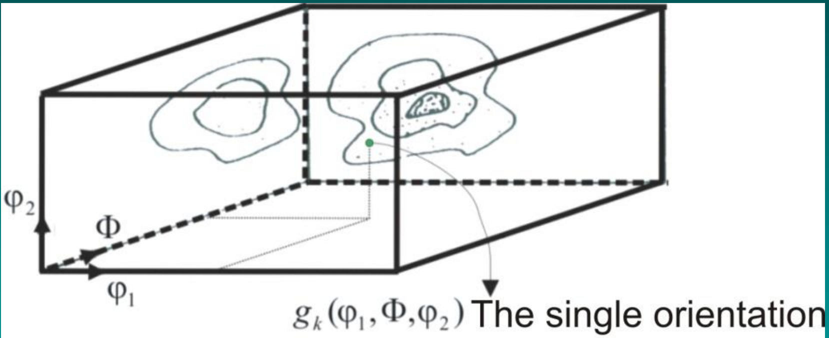

Schematic representation of the Euler space as the orientation space.

ODF – Orientation Distribution Function

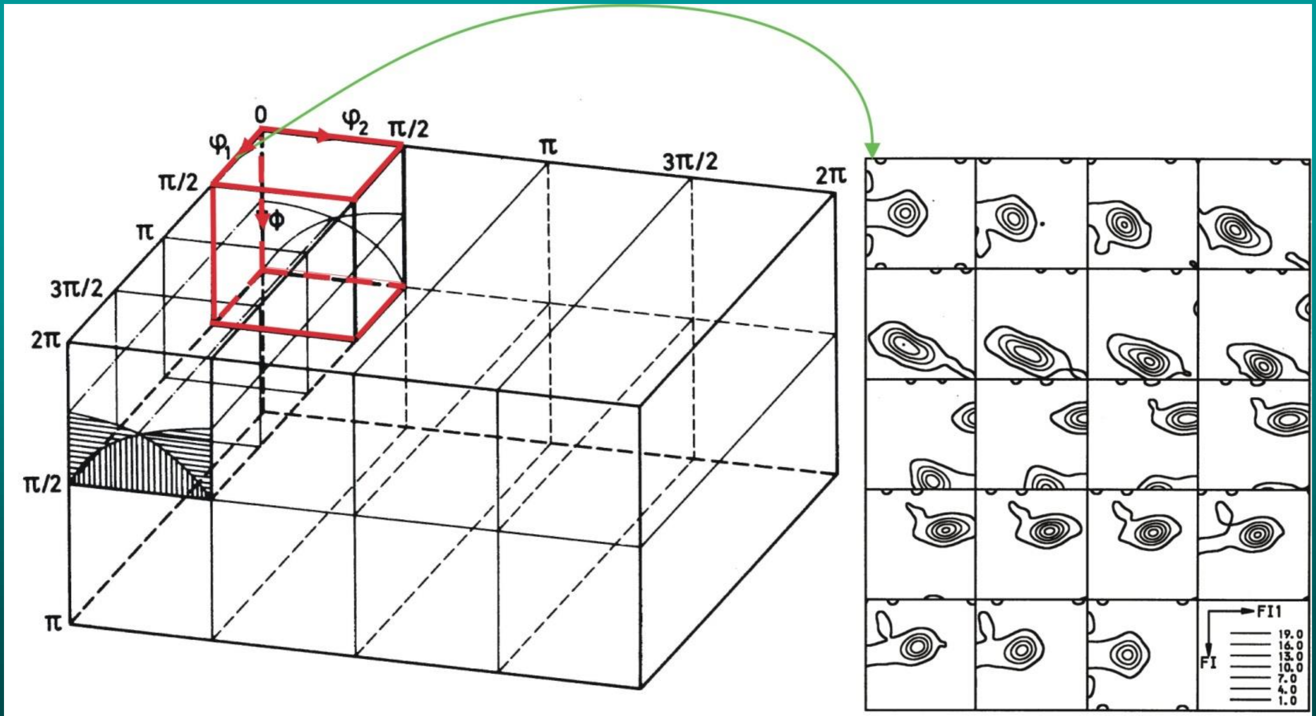

K. Sztwiertnia

Crystallographic orientation

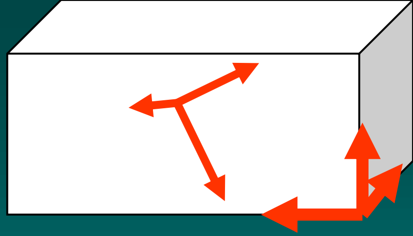

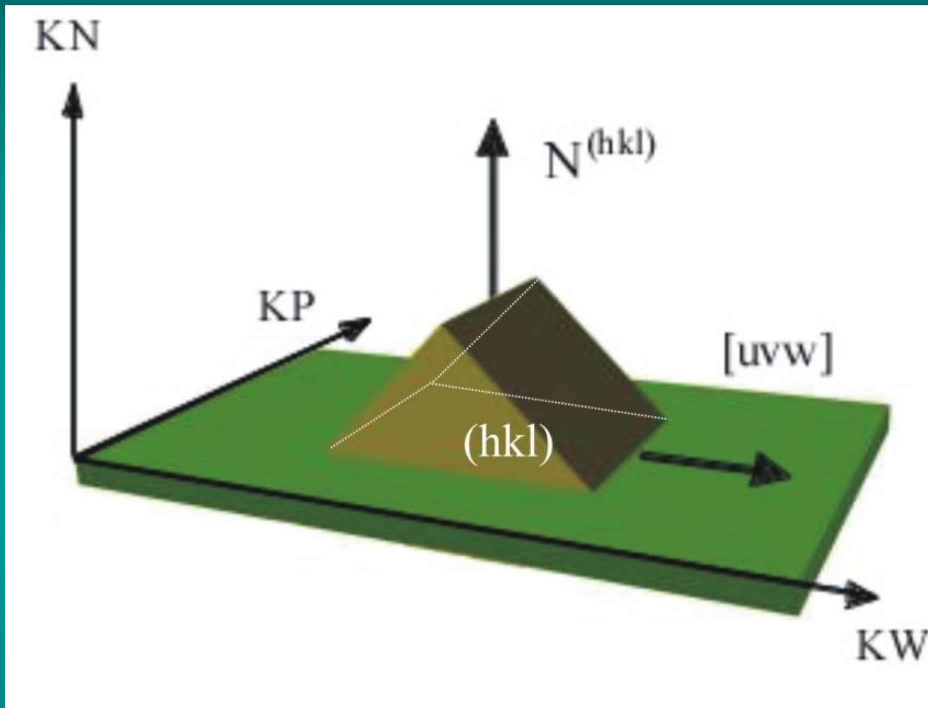

$$tg\phi \cos\varphi_2 = \frac{k}{l}$$

$$tg\varphi_2 = \frac{h}{k}$$

$$\cos\phi \, tg\varphi_1 = \frac{lw}{ku - hv}$$

The definition of crystallographic orientation with Miller indices (hkl) [uvw]; a relationship between indices and Euler angles for the cubic symmetry is shown.

K. Sztwiertnia

The geometry of interfaces

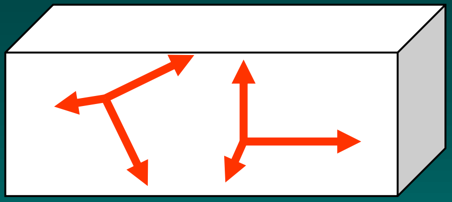

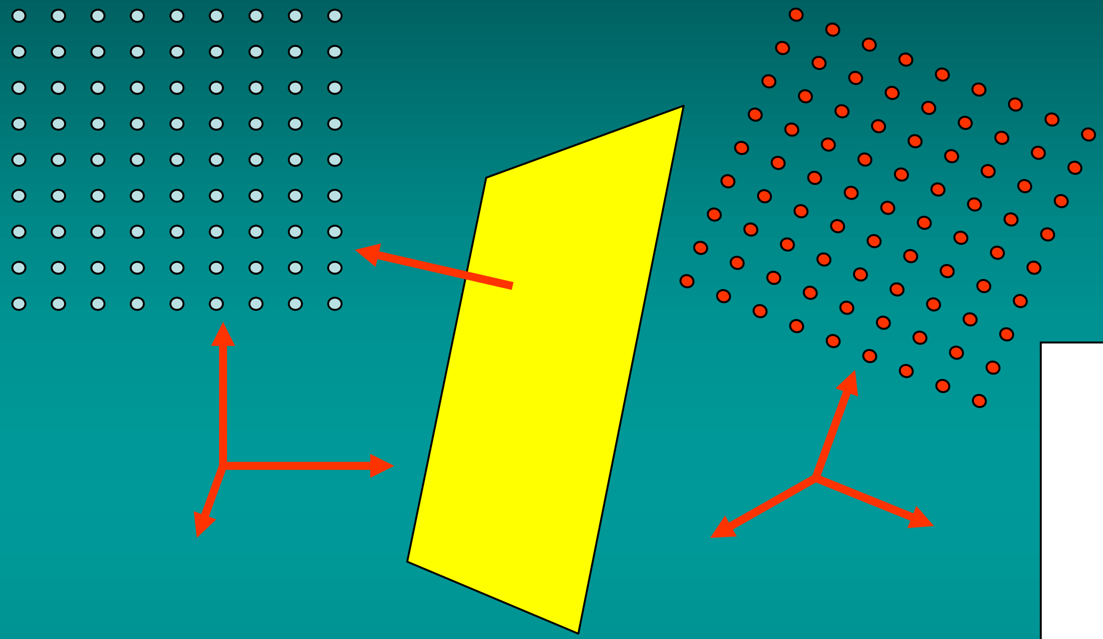

Geometry of the grain boundary:

- The rotation between two misoriented crystal lattices (misorientation),
- The orientation of the boundary plane.

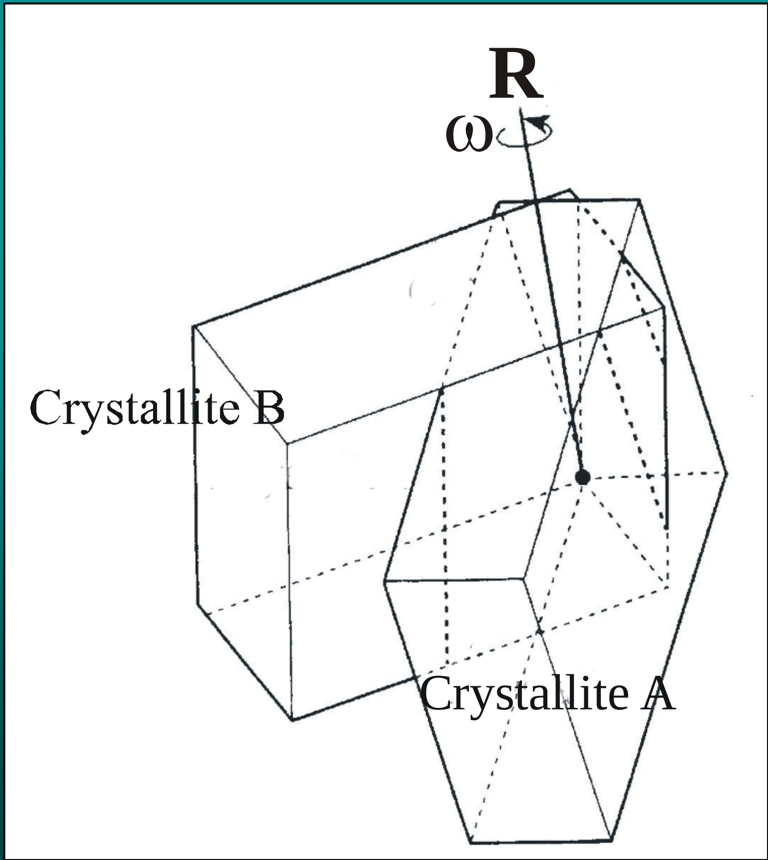

S_i

Misorientation between two crystallites

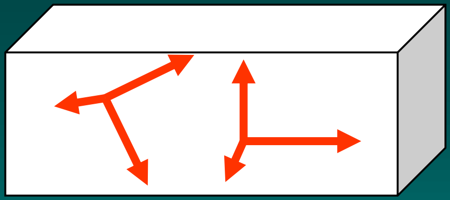

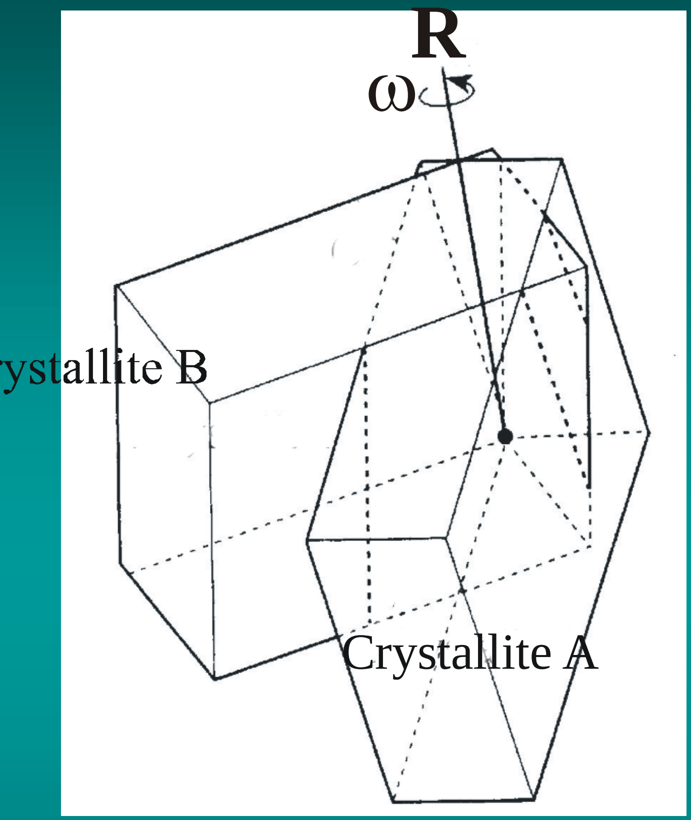

$$K_A = \Gamma_{AB} \cdot K_B$$

$$\Gamma_{AB}^{e} = S_i \cdot \Gamma_{AB} \cdot P_j$$
$$(i = 1, \ldots, M,\ j = 1, \ldots, N)$$

The misorientation is described by N*M symmetrically equivalent variants → for quantitative analysis of interfaces the misorientation should made be unique.

The rotation between two misoriented lattices may be described mathematically in several ways. These include the rotation matrix, the Euler angles, the axis/angle pair, the Rodrigues vector, the quaternion representation.

Misorientation between two crystallites

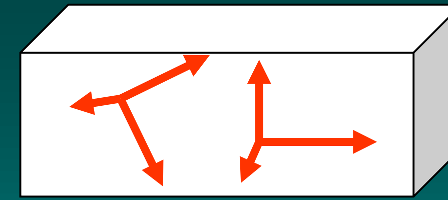

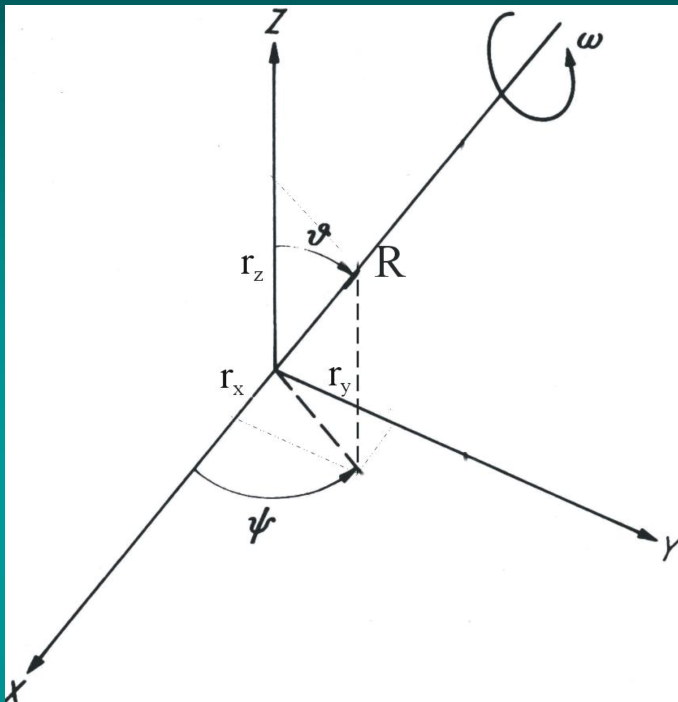

Rodrigues’ representation possesses certain properties of rectilinearity that make it relatively easy to construct asymmetric domains for different arrangements of crystallite symmetries.

The domains can be constructed in such a way that they contain rotations with smalest rotation angles.

The Rodrigues' parameters:

$$r_1 = r_x \cdot tg\left(\omega/2\right)$$

$$r_2 = r_y \cdot tg\left(\omega/2\right)$$

$$r_2 = r_z \cdot tg\left(\omega/2\right)$$

Frank, F.C. (1987) Orientation Mapping, *Metall. Trans. A*, 19A, 403-408.

K. Sztwiertnia

Asymmetric domains

(Rodrigues' representation)

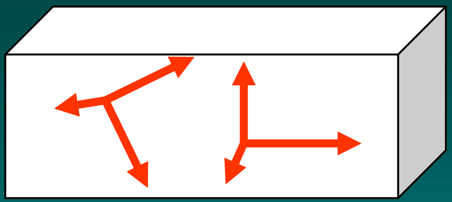

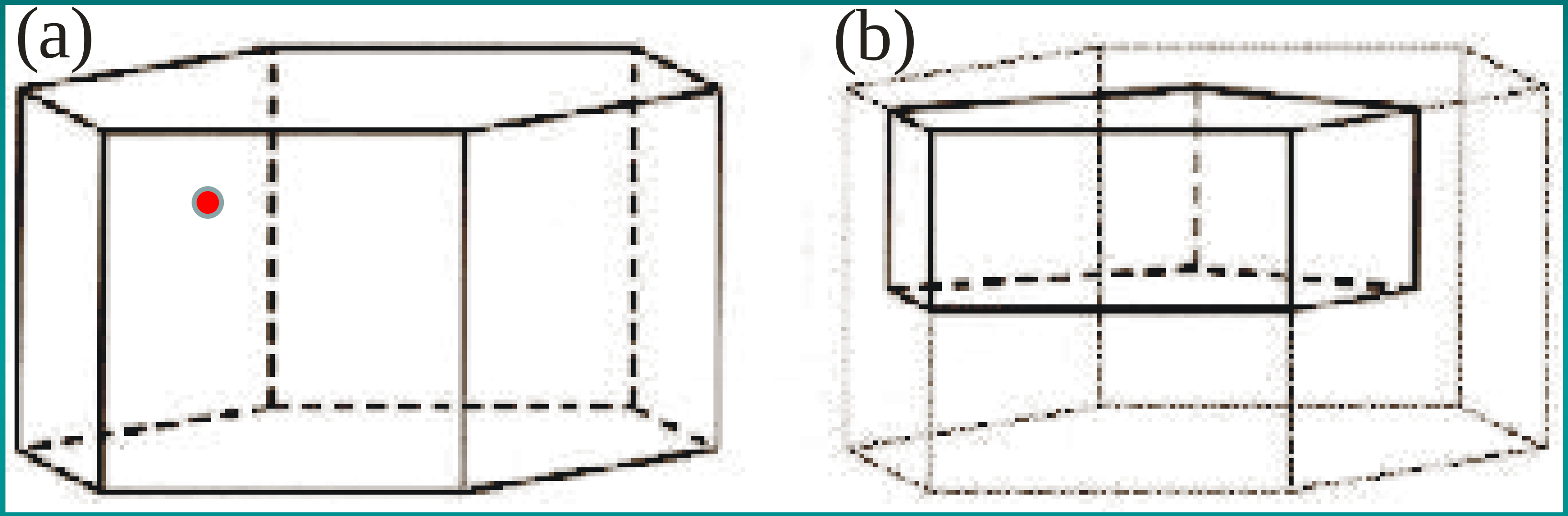

Schematic representation of the asymmetric domains for (D_3, C_1) (a) and (D_3, D_3) (b).

$$r_1, r_2, r_3 \rightarrow \begin{array}{c} (h_A\ k_A\ l_A) \parallel (h_B\ k_B\ l_B) \\ [u_A\ v_A\ w_A] \parallel [u_B\ v_B\ w_B] \end{array}$$

Morawiec, A. (2003) *Orientations and Rotations*, Springer Verlag, Berlin.

K. Sztwiertnia

The relationship between the microstructure, diffraction pattern and crystal orientation.

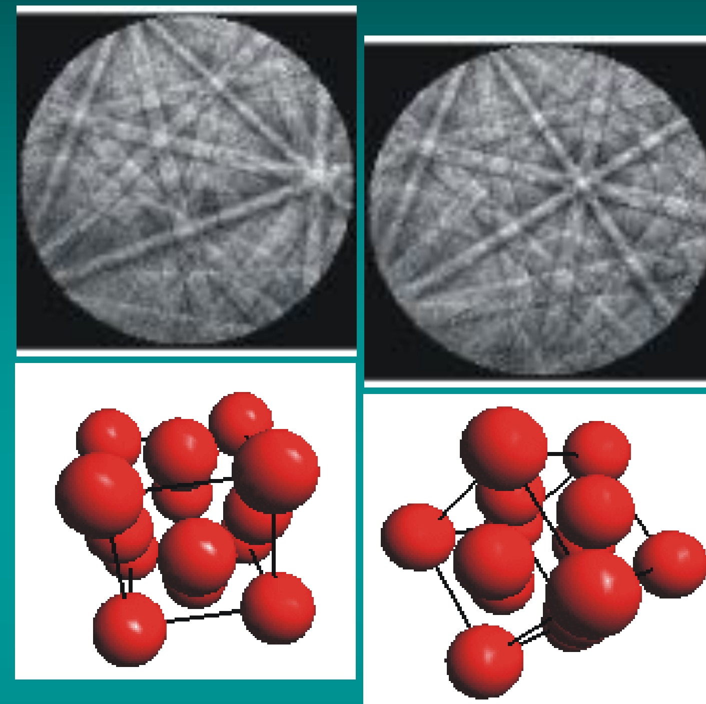

The microstructure of a stainless steel.

Crystal Orientation Mapping

Lines detection

⇓

Lines indexing

⇓

Crystal orientation

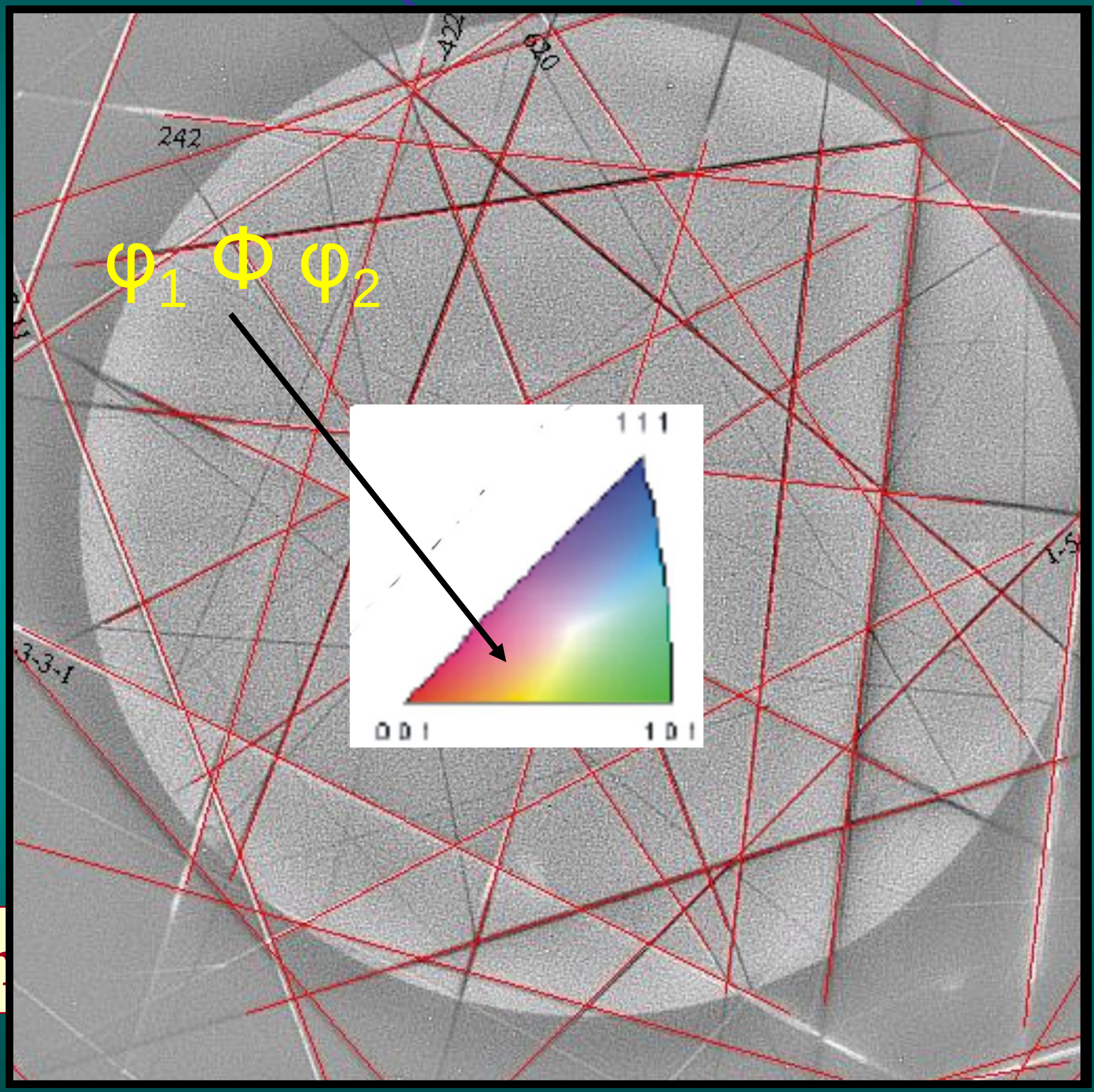

K. Sztwiertnia

Orientation mapping in SEM and TEM

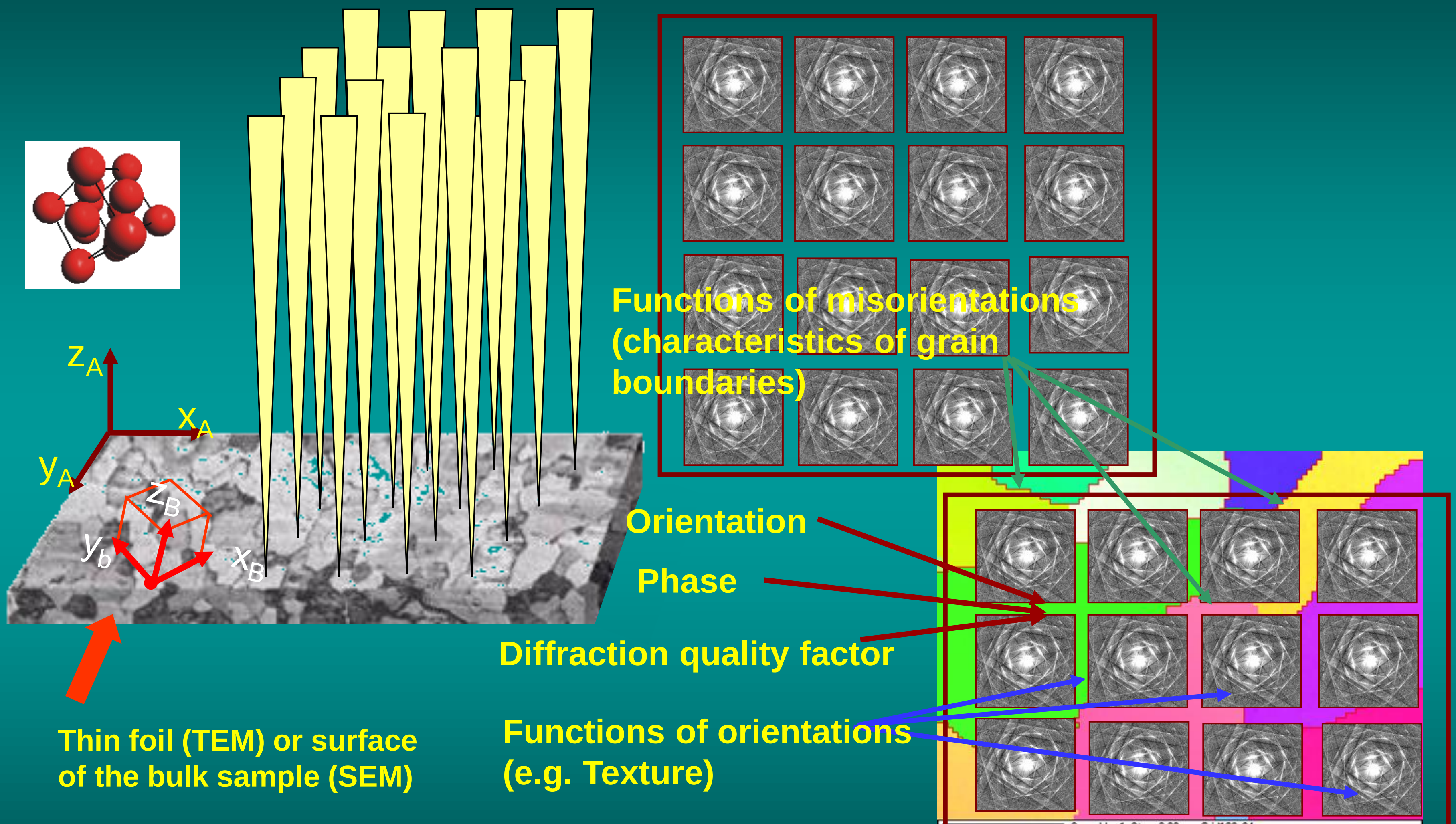

The orientation ☞ a rotation or a set of special rotations with the help of them a coordinate system K_A will be oriented parallel to K_B (K_A and K_B ☞ right-handed rectangular systems).

The orientation ☞ unambiguously characterised by three numbers combined in the symbol g.

$$K_B = g \cdot K_A$$

Orientation Microscopy

Spatial resolution ~ 100 nm (FEG)

Angular resolution > 0.5°

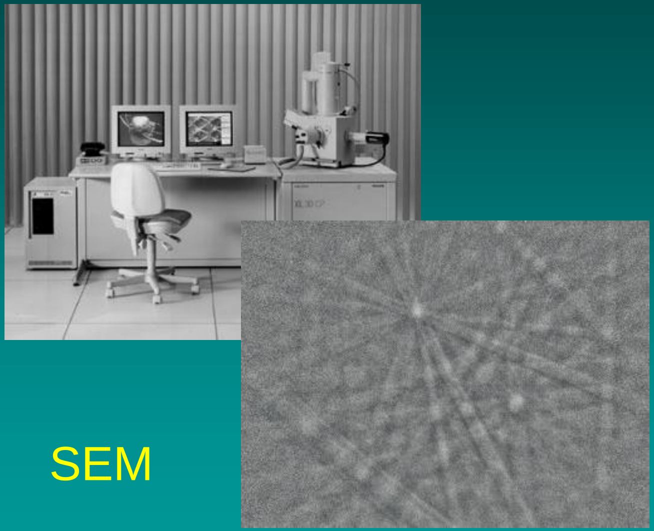

SEM

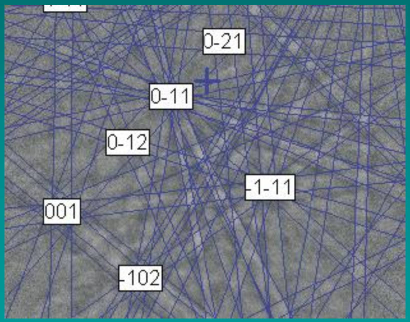

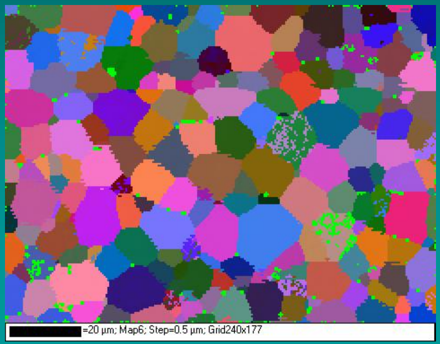

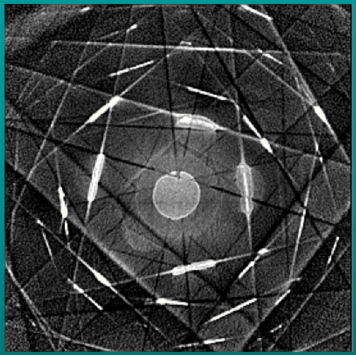

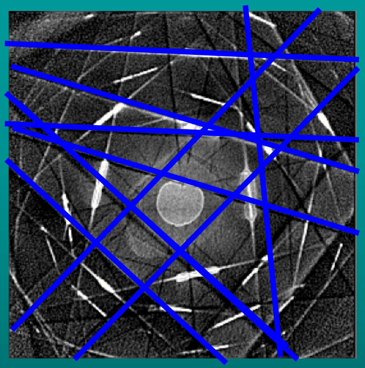

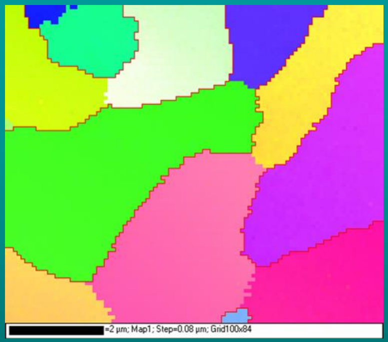

Spatial resolution ~ 10 nm

Angular resolution ~ 0.1°

TEM

Example I: Recrystallization of 6013 aluminum alloy

Alloy 6013, chemical composition (% by weight).

Mg	Si	Cu	Mn	Fe	Others	Al
1.15	1.0	1.1	0.3	0.5	0.15	Remainder

The investigations:

- Analysis of microstructure in a state after deformation. Measurement of local crystallographic orientations (TEM).
- Calorimetric measurements of recrystallization (non-isothermal method, differential calorimeter).
- Analysis of microstructures and local orientation distributions in samples annealed in a calorimeter to the various recrystallization stages.

K. Sztwiertnia, J. Morgiel, E. Bouzy, Arch. Metall. Mater., 50 (2005) 119.

Example I:Recrystallization of 6013 aluminium alloy

Microstructure of 75% cold-rolled 6013 alloy, longitudinal section, TEM.

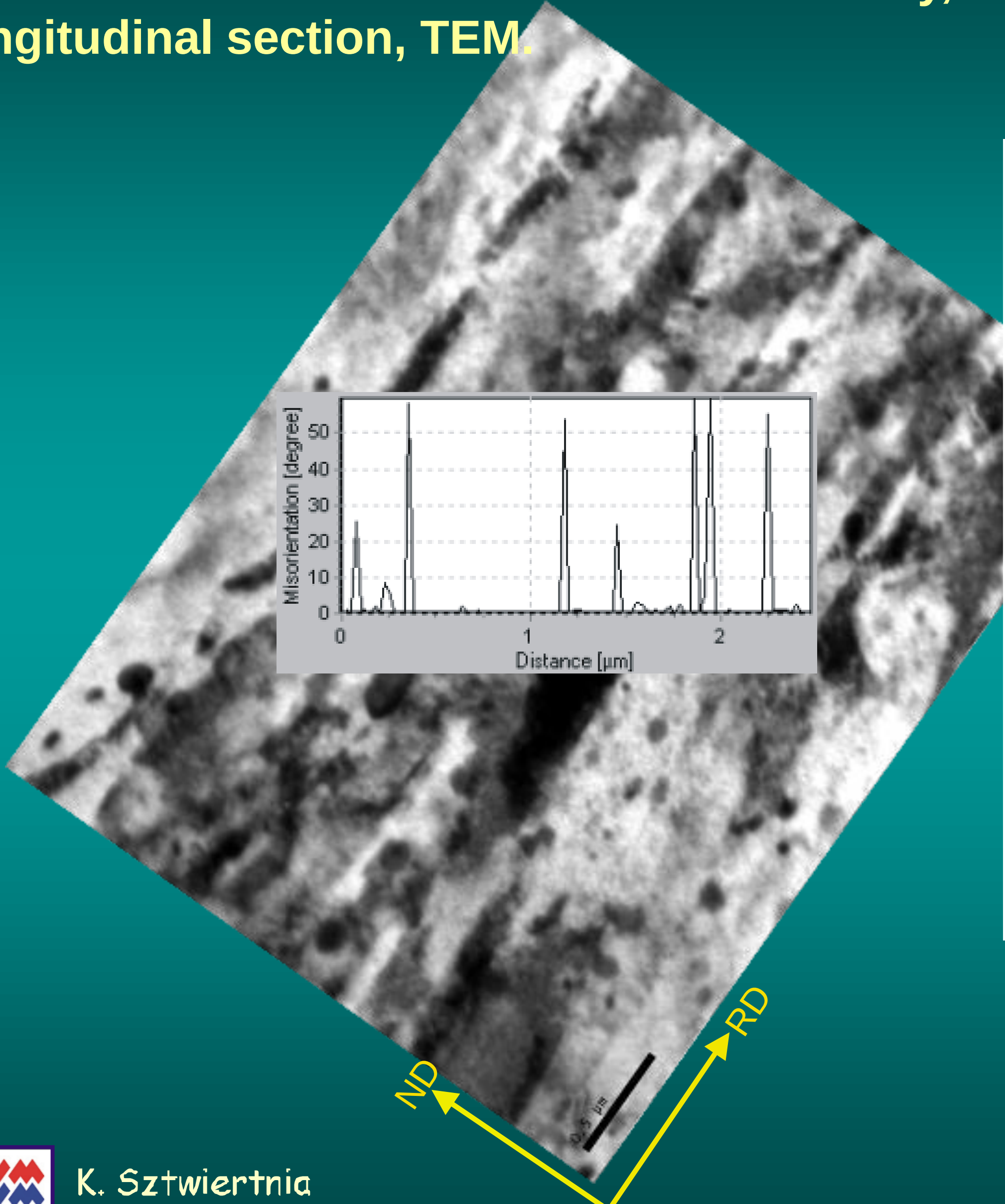

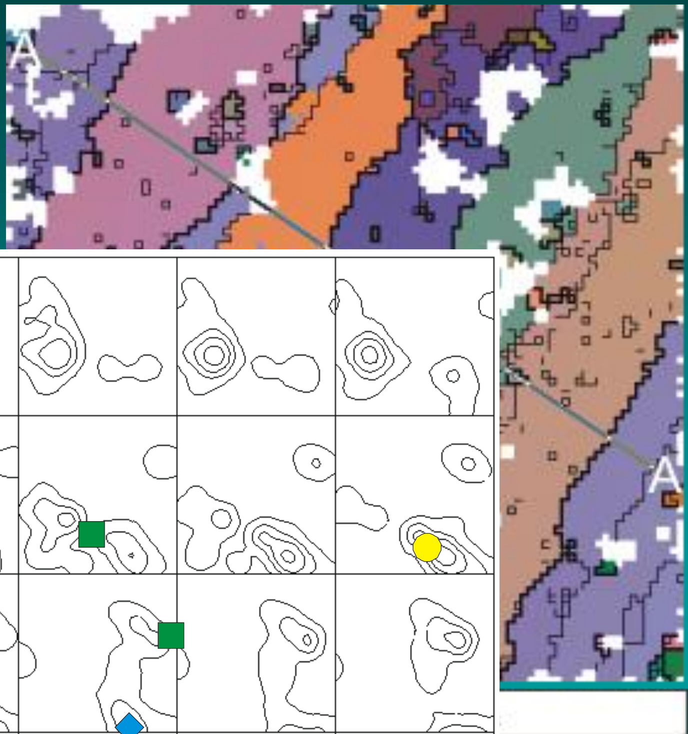

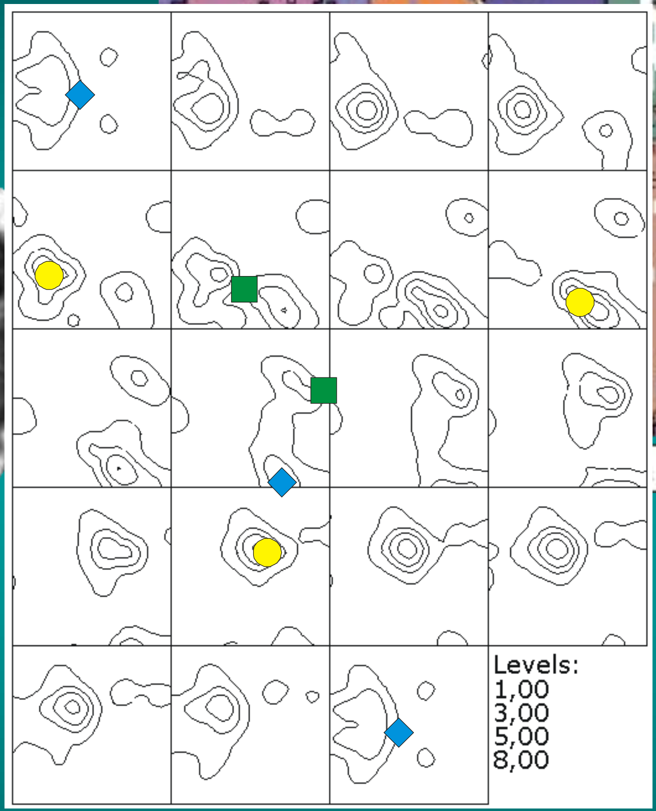

S={123}<634>,

Copper={112}<111>,

Brass={011}<211>.

K. Sztwiertnia

Example I:Recrystallization of 6013 aluminium alloy

Microstructure of 90% cold-rolled 6013 aluminum alloy, *in-situ* annealing, longitudinal section, **TEM (**spatial resolution ~ 10 nm).

.

Orientation topography in the area of the deformation zone

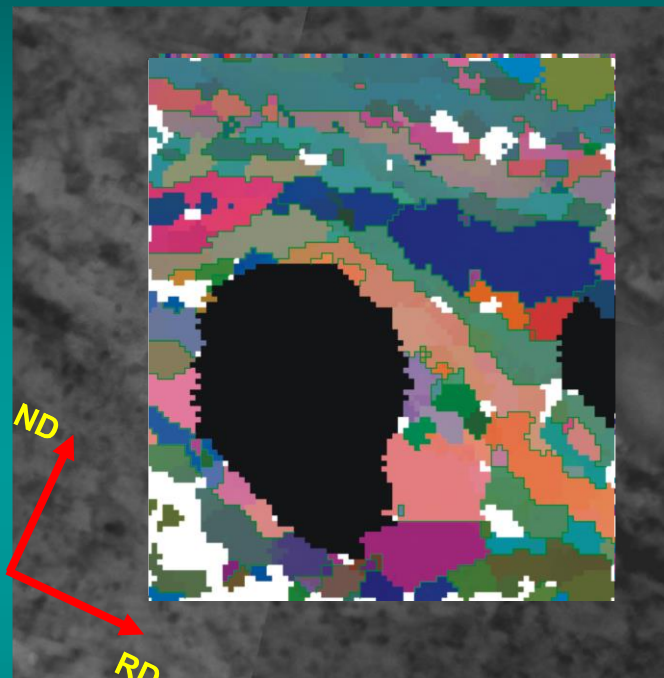

1 μm , Step= 30 nm, Grid 100 x 100

Orientation topography in the area of the deformation zone after heating *in-situ* in TEM

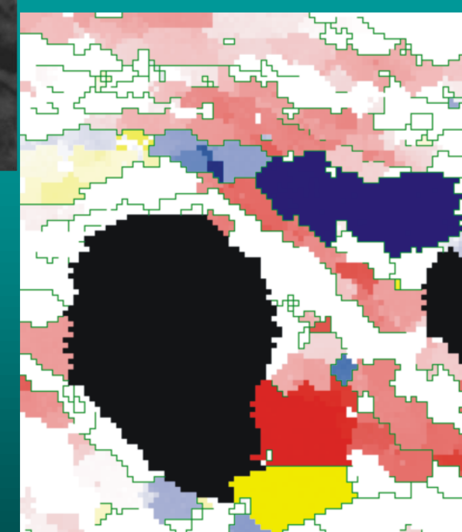

M. Bieda, K.Sztwiertnia, A. Korneva, T. Czeppe, R. Orlicki, Solid State Phenomena, 16 (2010) 13-18.

Example I:Recrystallization of 6013 aluminium alloy

Rodrigues' representation r_1, r_2, r_3, cross-section r_3=const., asymmetric domain (O, O).
(**H**igh **A**ngle **G**rain **B**oundaries only; $\omega > 15°$).

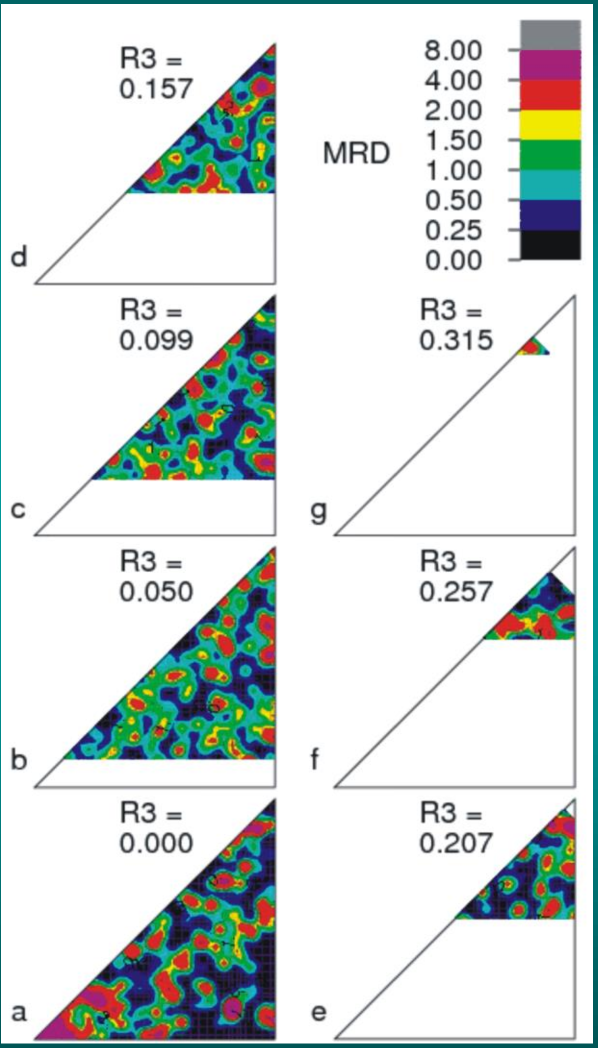

Misorientation distribution between orientations of crystallites in deformation zones (before annealing) and new grains growing in the same places; 75% cold-rolled 6013 aluminum alloy

Misorientation distribution between orientations of crystallites in deformation zones (before annealing) and new grains growing in the same places; 90% cold-rolled 6013 aluminum alloy

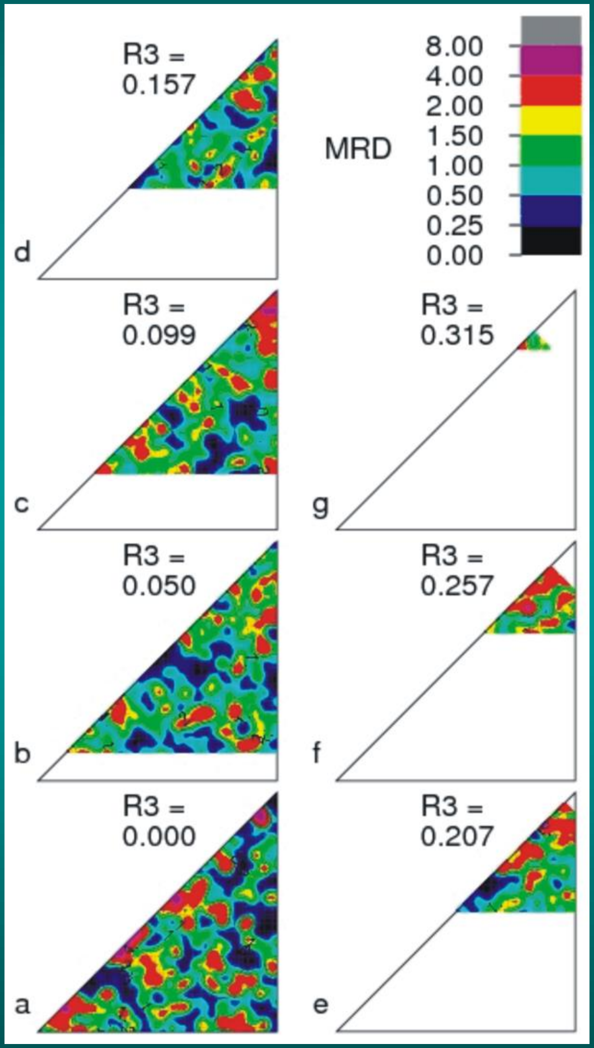

M. Bieda, K.Sztwiertnia, A. Korneva, T. Czeppe, R. Orlicki, Solid State Phenomena, 16 (2010) 13-18.

Example I:Recrystallization of 6013 aluminium alloy

Power difference, representing release of stored energy from 75% and 90% cold-rolled 6013 alloy, as a function of annealing temperature.

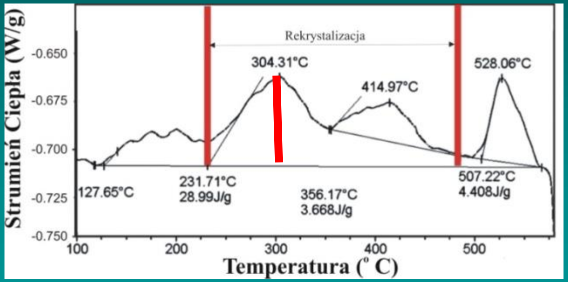

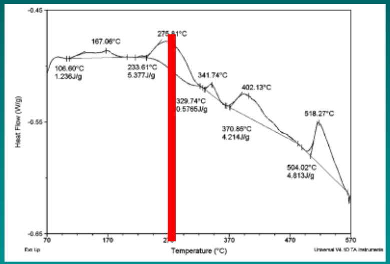

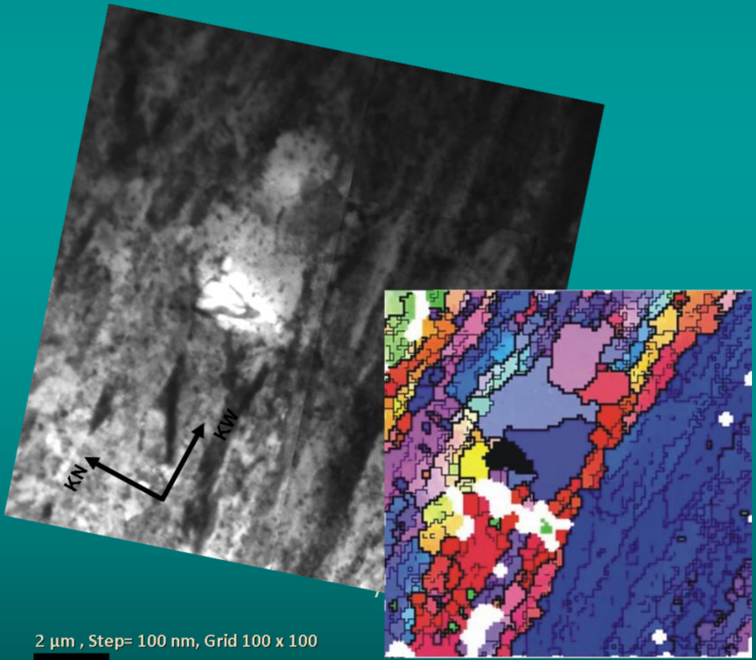

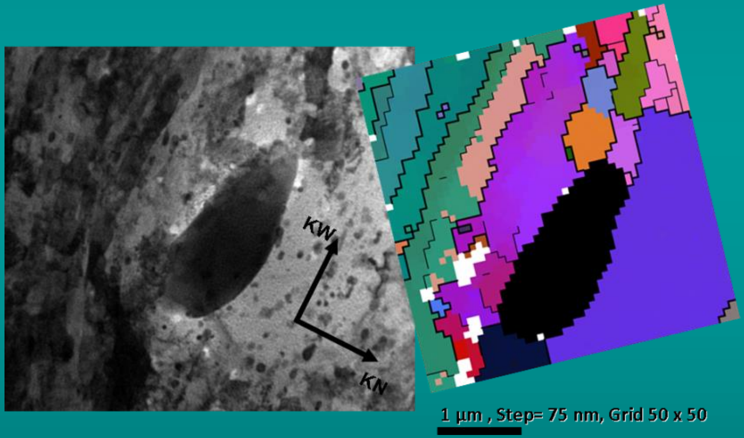

Microstructures of 6013 alloy, 75% and 90% cold-rolled and subsequently heated in the calorimeter to 300^0C and 280^0C, CBED/TEM, longitudinal section.

Example I:Recrystallization of 6013 aluminium alloy

Power difference, representing release of stored energy from 75% cold-rolled 6013 alloy, as a function of annealing temperature.

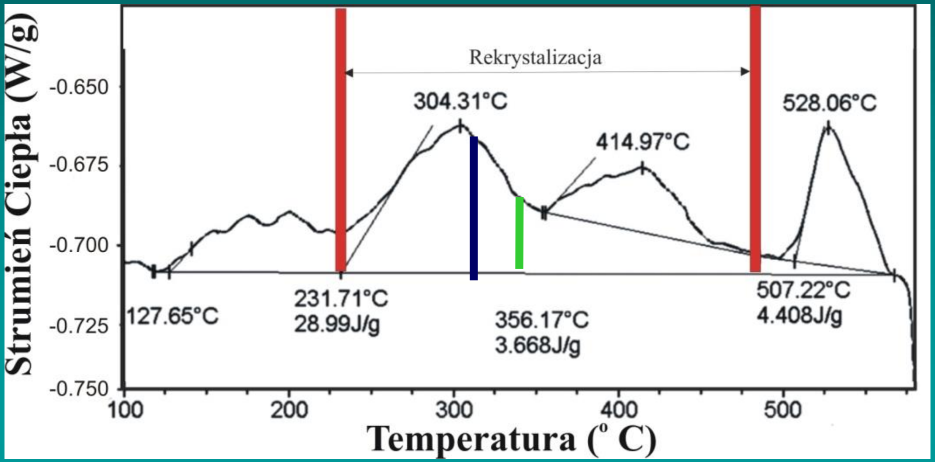

Microstructures of 6013 alloy, 75% cold-rolled and subsequently heated in the calorimeter to 330^{0}C and 350^{0}C, EBSD/SEM, longitudinal section.

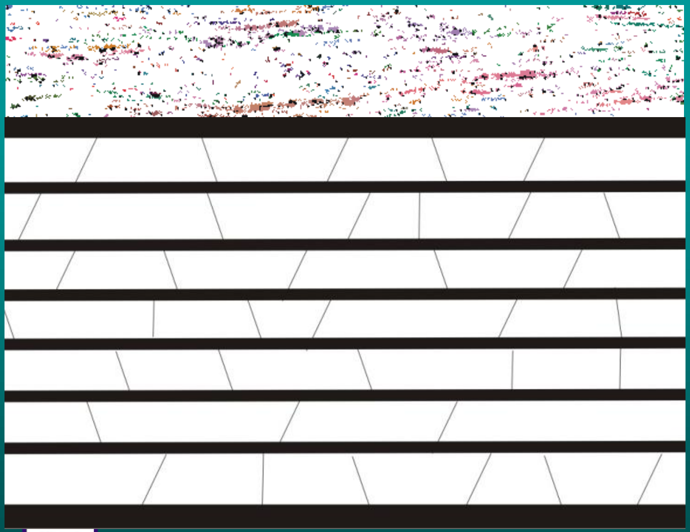

K. Sztwiertnia

M. Bieda, K.Sztwiertnia, A. Korneva, T. Czeppe, R. Orlicki, Solid State Phenomena, 16 (2010) 13-18.

Example I:Recrystallization of 6013 aluminium alloy

Power difference, representing release of stored energy from 75% cold-rolled 6013 alloy, as a function of annealing temperature.

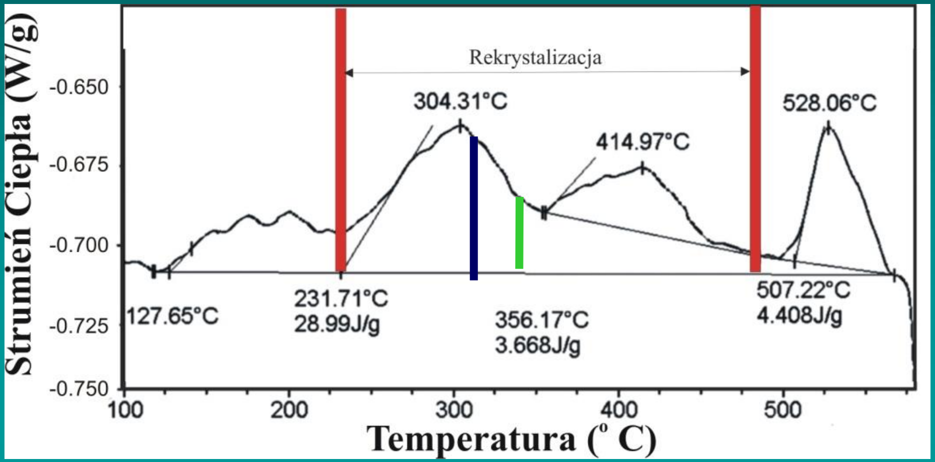

Microstructures of 6013 alloy, 75% cold-rolled and subsequently heated in the calorimeter to 480^0C, EBSD/SEM, longitudinal section.

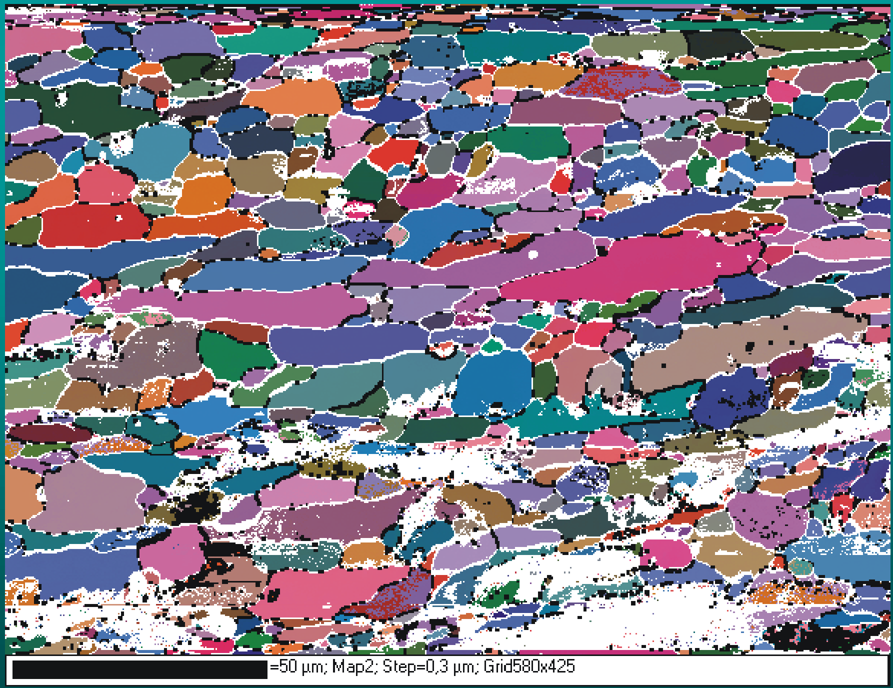

K. Sztwiertnia

M. Bieda, K.Sztwiertnia, A. Korneva, T. Czeppe, R. Orlicki, Solid State Phenomena, 16 (2010) 13-18.

Example II, Orientation mapping applied to gradient materials

Hard magnetic Fe-Cr-Co alloy was subjected to severe plastic deformation by complex two-step loading.

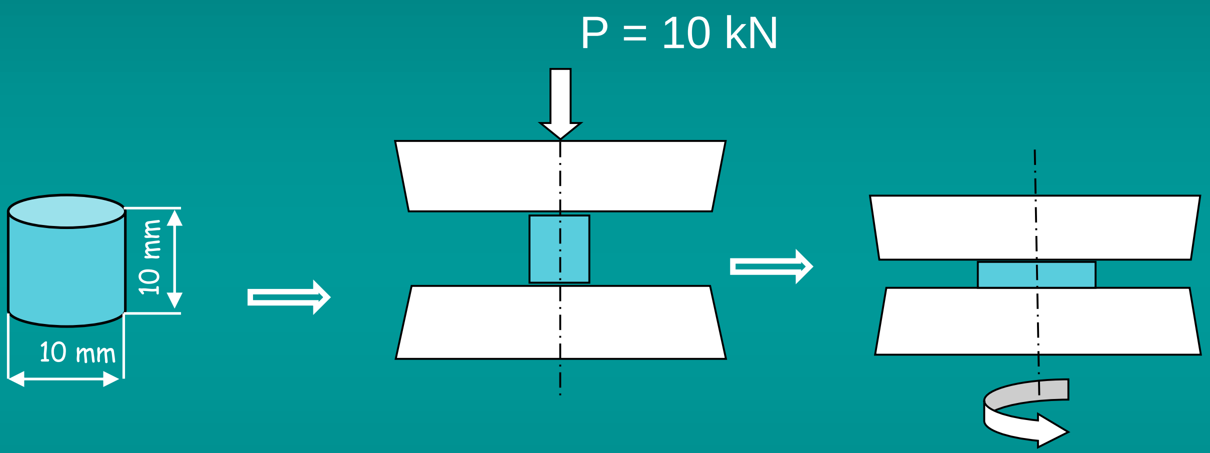

Schema of deformation by upsetting and subsequent torsion.

A. V. Korneva, M. Bieda, G.F. Korznikova and K. Sztwiertnia, Arch. Metall., 51 (2006) 69.

Example II, Orientation mapping applied to gradient materials

The microstructure of the hard magnetic Fe-Cr-Co alloy after severe plastic deformation.

The top part of the sample

The middle part of the sample

The bottom part of the sample

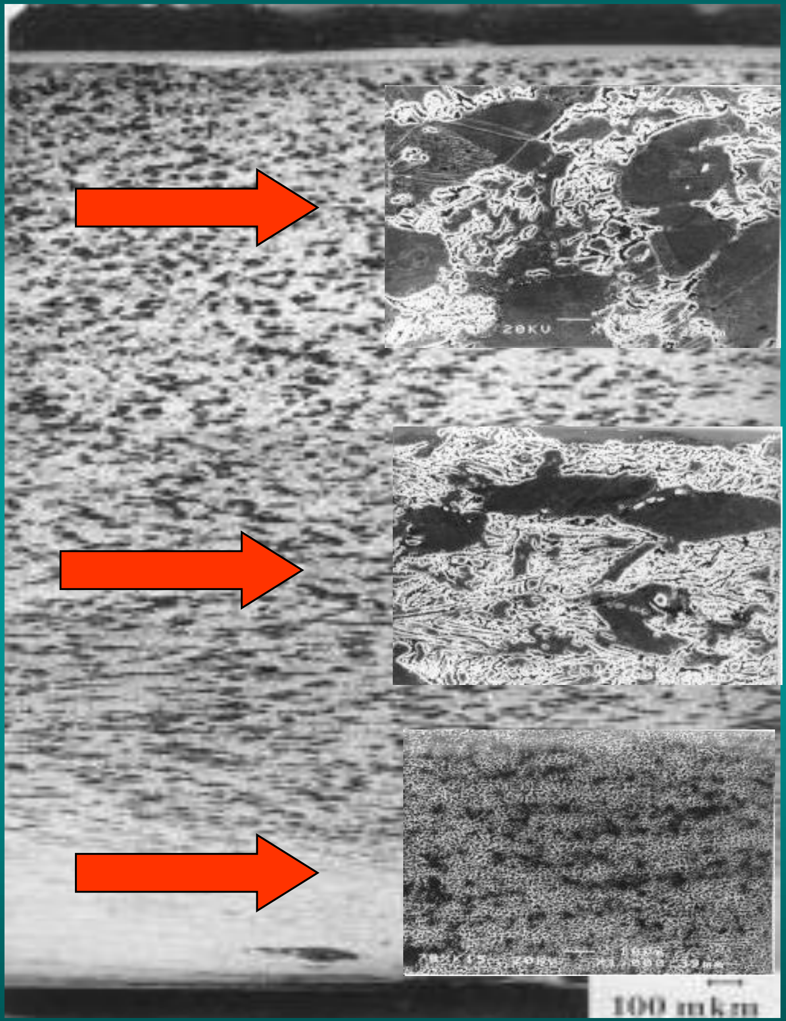

A. Korneva, M. Bieda, G. Korznikowa, K. Sztwiertnia, A. Korznikov, International Journal of Materials Research, 99 (2008) 991-998.

Example II, Orientation mapping applied to gradient materials

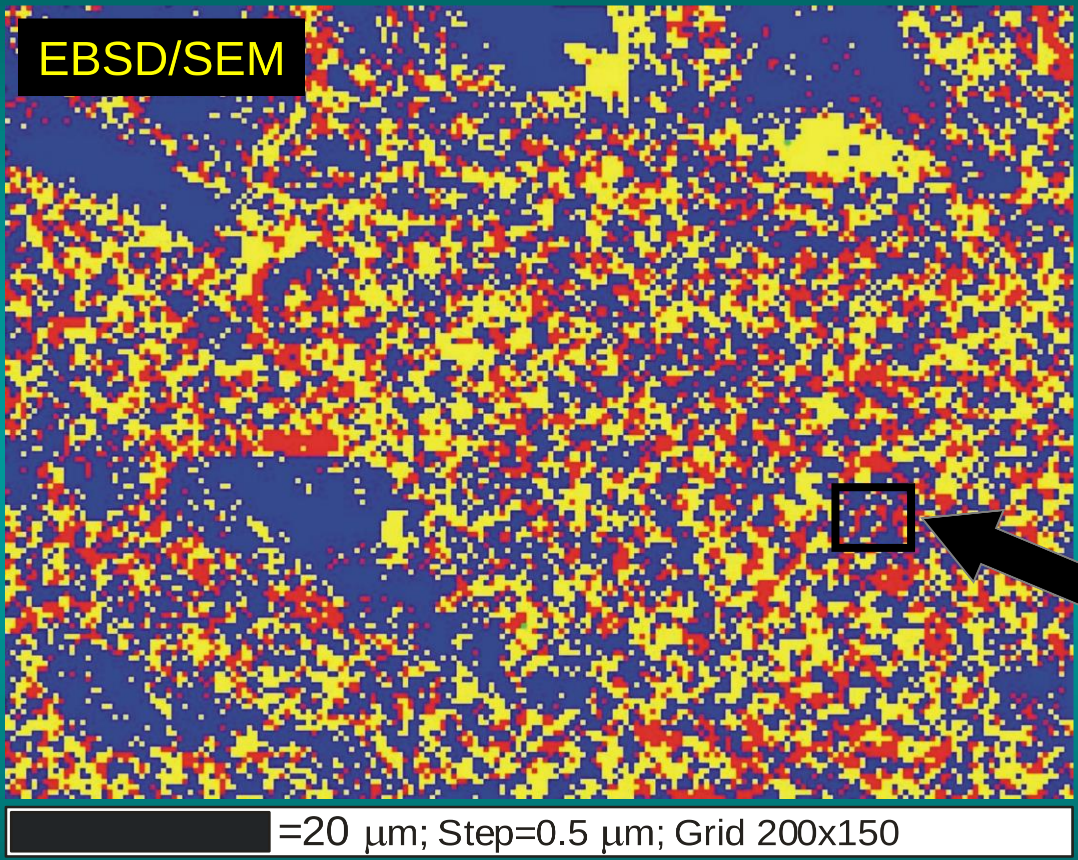

- α (bcc)
- γ (fcc)
- σ-(tetragonal)

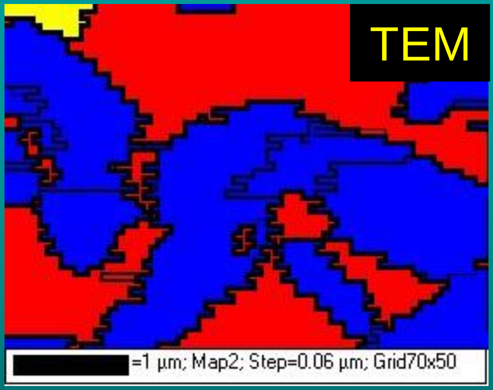

The top part of the sample, deformed at 700 ºC, EBSD/SEM.

Example II, Orientation mapping applied to gradient materials

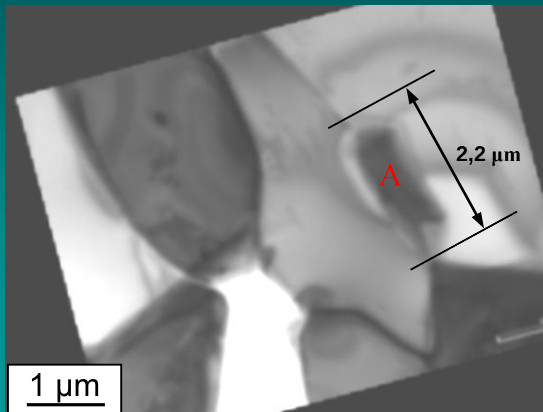

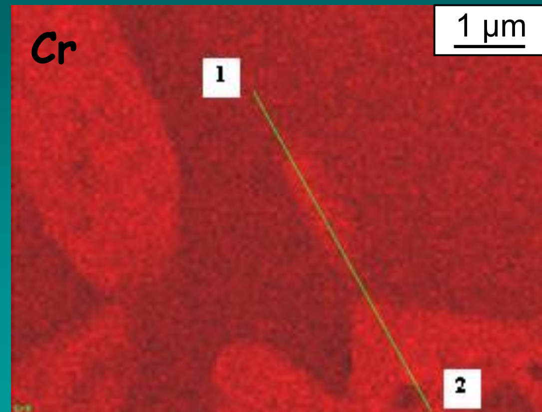

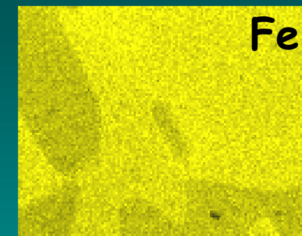

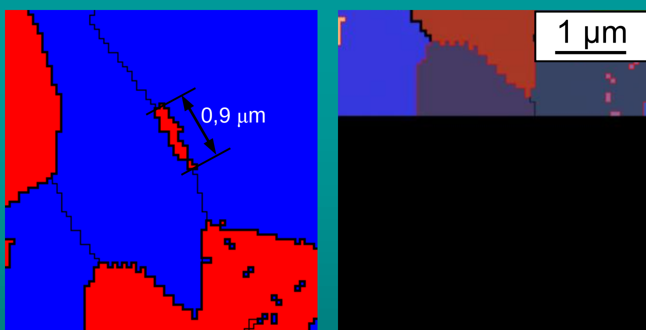

α phase σ phase

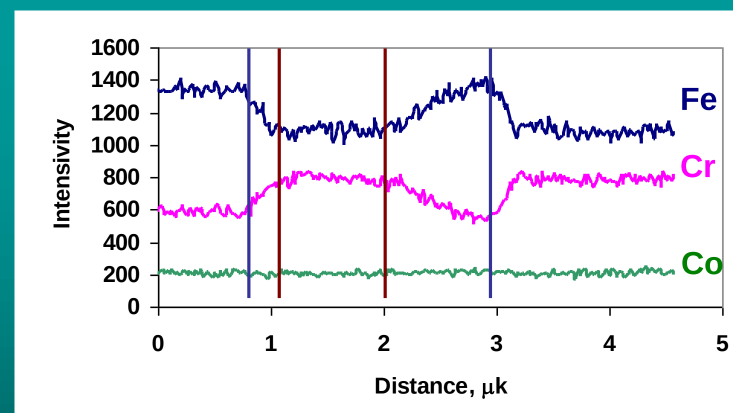

The bottom part of the sample, deformed at 800 ºC and then annealed 30 min at 450 ºC, TEM.

A. Korneva, M. Bieda, G. Korznikova, A. Korznikov, K. Sztwiertnia, International Journal of Materials Research, 102 (2011) 32.

Example III: Orientation mapping applied to composites.

Misorientation characteristic of interphase boundaries.
(Al_2O_3/ WC, SEM).

Example III: Microstructure of Al_2O_3/ WC composite (ESEM/EBSD phase map)

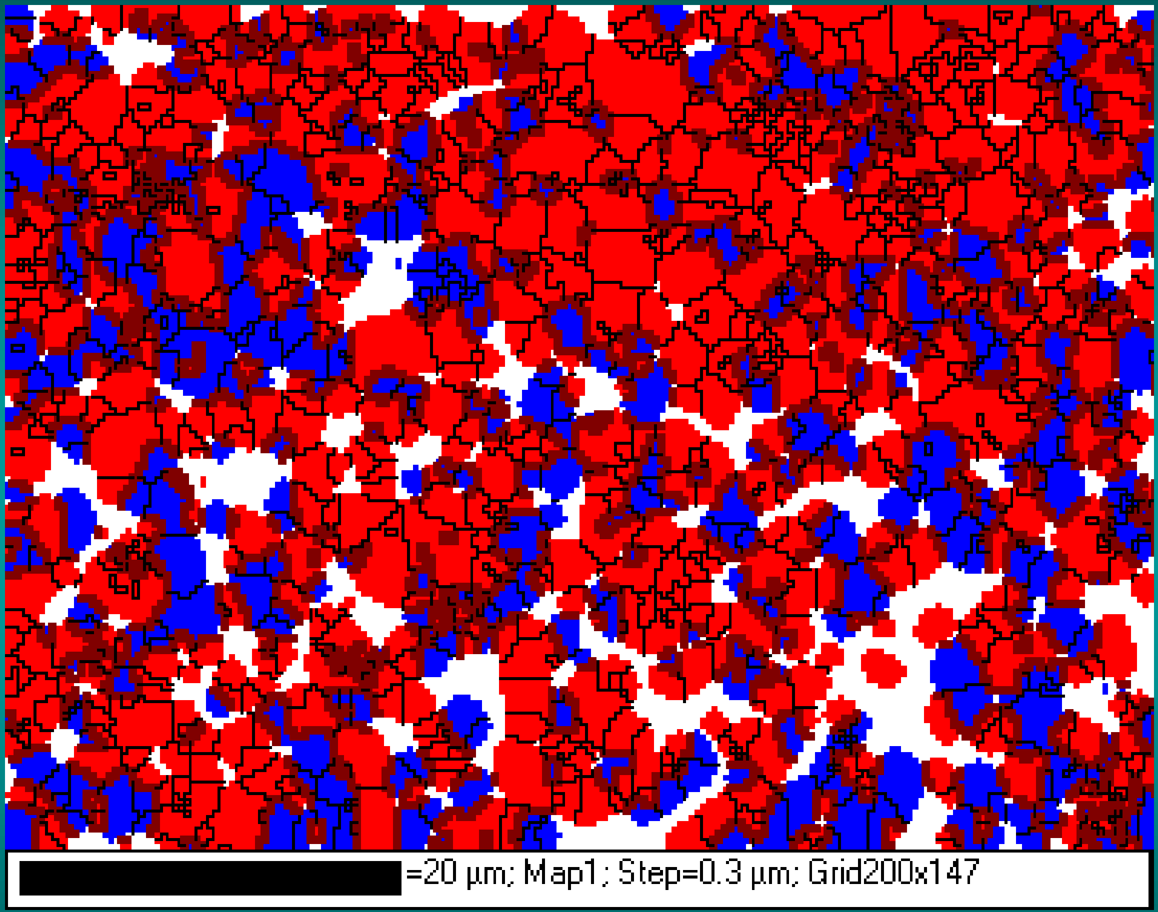

Al_2O_3 grains – red, WC grains – blue, white regions – not indexed; thick lines – Al_2O_3/WC interphase boundaries, thin lines – grain boundaries.

K. Sztwiertnia, M. Faryna, G. Sawina, Journal of the European Ceramic Society, 26 (2006) 2973.

Example III: Microstructure of Al_2O_3/ WC composite (ESEM/EBSD orientation map)

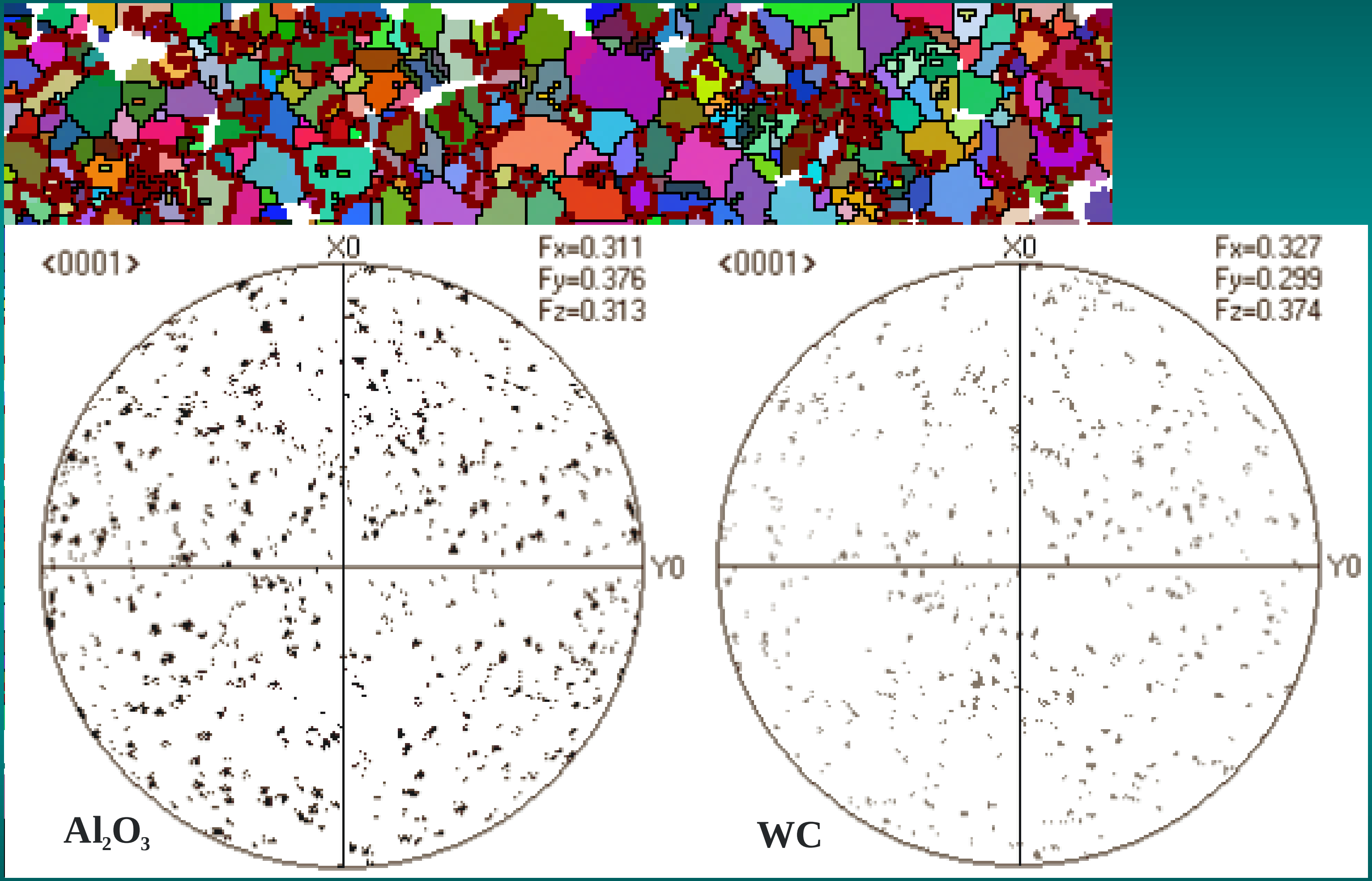

Stereographic projections of directions <0001> in Al_2O_3 grains and WC grains, respectively.

K. Sztwiertnia, M. Faryna, G. Sawina, Journal of the European Ceramic Society, 26 (2006) 2973.

Example III: Misorientation Distribution Function (Al_2O_3/ WC)

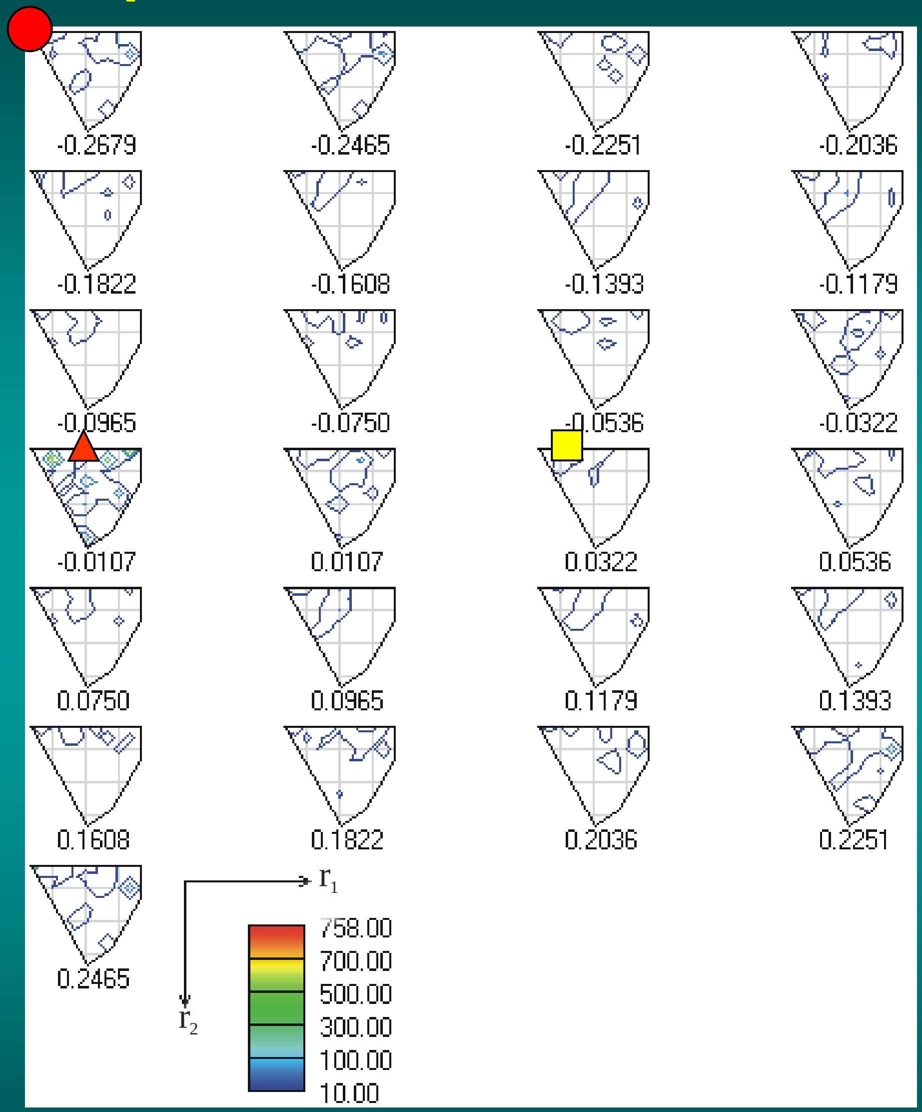

$(0\bar{1}11)\,WC \parallel (1\bar{1}05)\,Al_2O_3$

$[11\bar{2}3]\,WC \parallel [\bar{2}3\bar{1}1]\,Al_2O_3$

$(0\bar{1}11)\,WC \parallel (\bar{1}011)\,Al_2O_3$

$[2\bar{1}\bar{1}0]\,WC \parallel [01\bar{1}1]\,Al_2O_3$

$(0001)\,WC \parallel (0001)\,Al_2O_3$

$[11\bar{2}0]\,WC \parallel [10\bar{1}0]\,Al_2O_3$

MDF between Al_2O_3 and WC grains; Rodrigues' representation r_1, r_2, r_3, cross-section r_3=const., asymmetric domain (D_6, D_3).

K. Sztwiertnia, M. Faryna, G. Sawina, Journal of the European Ceramic Society, 26 (2006) 2973.

Example III: Misorientation Distribution Function (Al_2O_3/ WC)

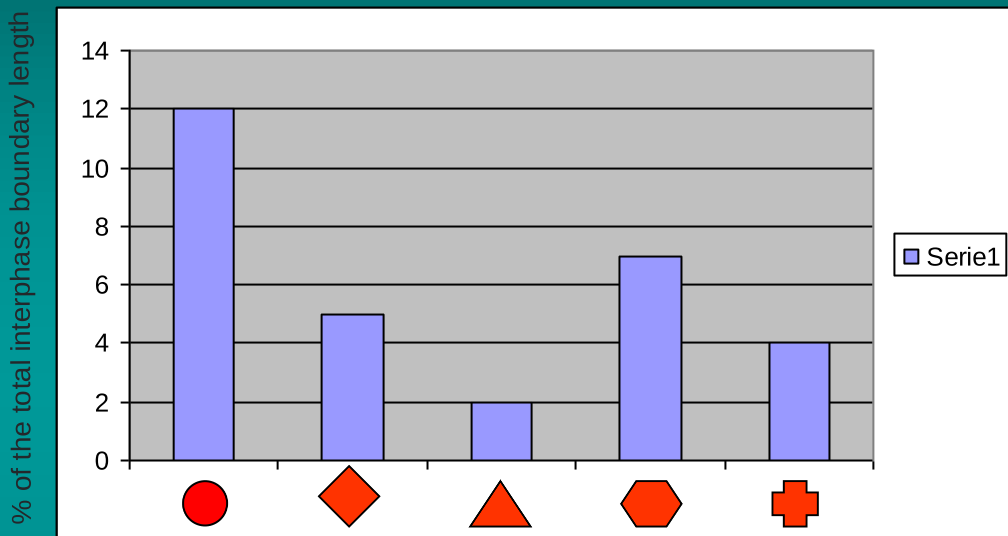

$$(0\,0\,0\,1)\,WC \parallel (0\,0\,0\,1)\,Al_2O_3$$
$$[1\,1\,\bar{2}\,0]\,WC \parallel [1\,0\,\bar{1}\,0]\,Al_2O_3$$

$$(1\,0\,\bar{1}\,0)\,WC \parallel (1\,0\,\bar{1}\,0)\,Al_2O_3$$
$$[0\,0\,0\,\bar{1}]\,WC \parallel [\bar{1}\,3\,\bar{2}\,\bar{2}]\,Al_2O_3$$

$$(1\,0\,\bar{1}\,0)\,WC \parallel (1\,0\,\bar{1}\,0)\,Al_2O_3$$
$$[0\,0\,0\,\bar{1}]\,WC \parallel [\bar{4}\,9\,\bar{5}\,2]\,Al_2O_3$$

$$(2\,\bar{1}\,\bar{1}\,0)\,WC \parallel (2\,\bar{1}\,\bar{1}\,0)\,Al_2O_3$$
$$[0\,0\,0\,\bar{1}]\,WC \parallel [0\,1\,\bar{1}\,0]\,Al_2O_3$$

$$(3\,\bar{1}\,\bar{2}\,0)\,WC \parallel (3\,\bar{1}\,\bar{2}\,0)\,Al_2O_3$$
$$[0\,1\,\bar{1}\,\overline{12}]\,WC \parallel [\bar{1}\,9\,\bar{8}\,\bar{1}]\,Al_2O_3$$

The crystallographic relationships correspond respectively to: 12%, 5%, 2%, 7% and 4% of the total WC/ Al_2O_3 interphase boundary length.

K. Sztwiertnia, M. Faryna, G. Sawina, Journal of the European Ceramic Society, 26 (2006) 2973.

Example IV: EBSD Image Quality Maps

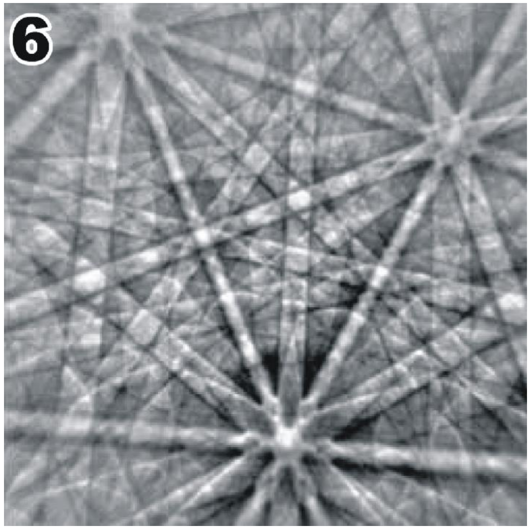

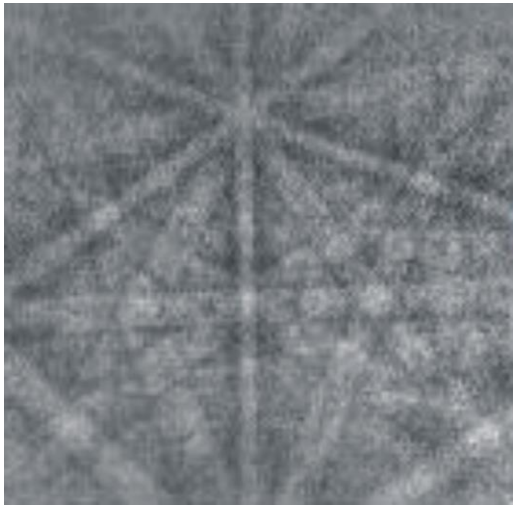

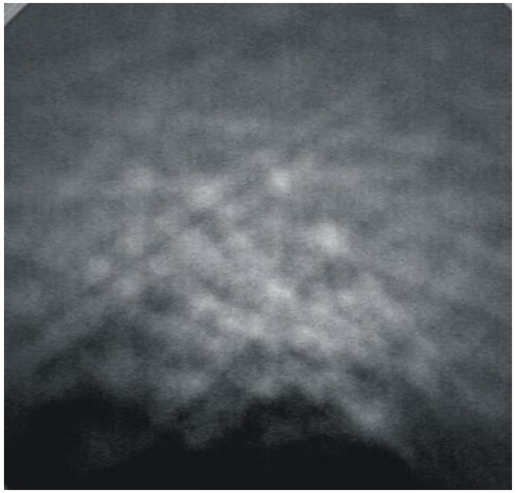

Diffraction patterns from places with various dislocation densities (Al_2O_3).

The additional data contained in the diffraction image can be used, e.g. for differentiation of material areas with different dislocation density.

Definition of different types of stresses at various spatial scales

Scale of the first order stresses

(the macrostress σ_{ij}^{M} is the mean value over V_A volume)

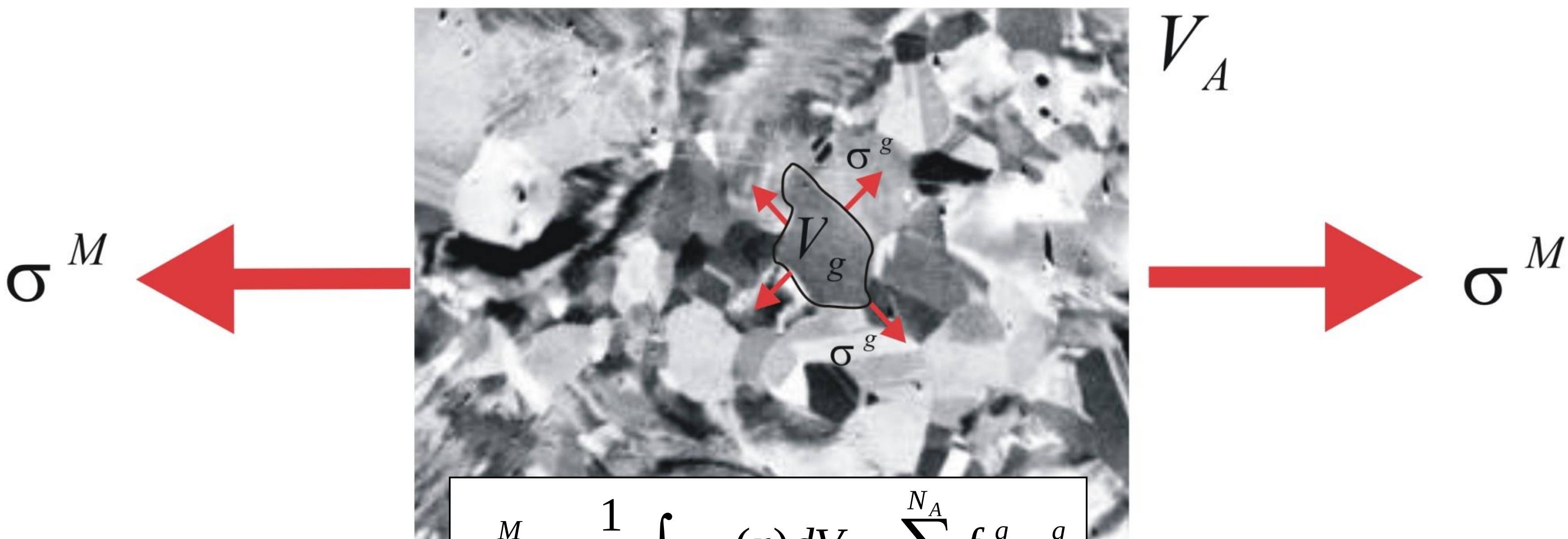

$$\boxed{\sigma_{ij}^{M} = \frac{1}{V_A}\int_{V_A}\sigma_{ij}(r)dV = \sum_{g}^{N_A} f^{g}\sigma_{ij}^{g}}$$

where: N_A - total number of grains $\sigma_{ij}(r)$ - local stress at *r* position

$f^{g} = \frac{V_g}{V_A}$ and σ_{ij}^{g} - the volume fraction and the mean stress for grain *g* having volume V_g

Definition of different types of stresses at various spatial scales

Scale of the second order stresses

(σ_{ij}^{g} is the mean stress for the volume V_g of the g– th grain)

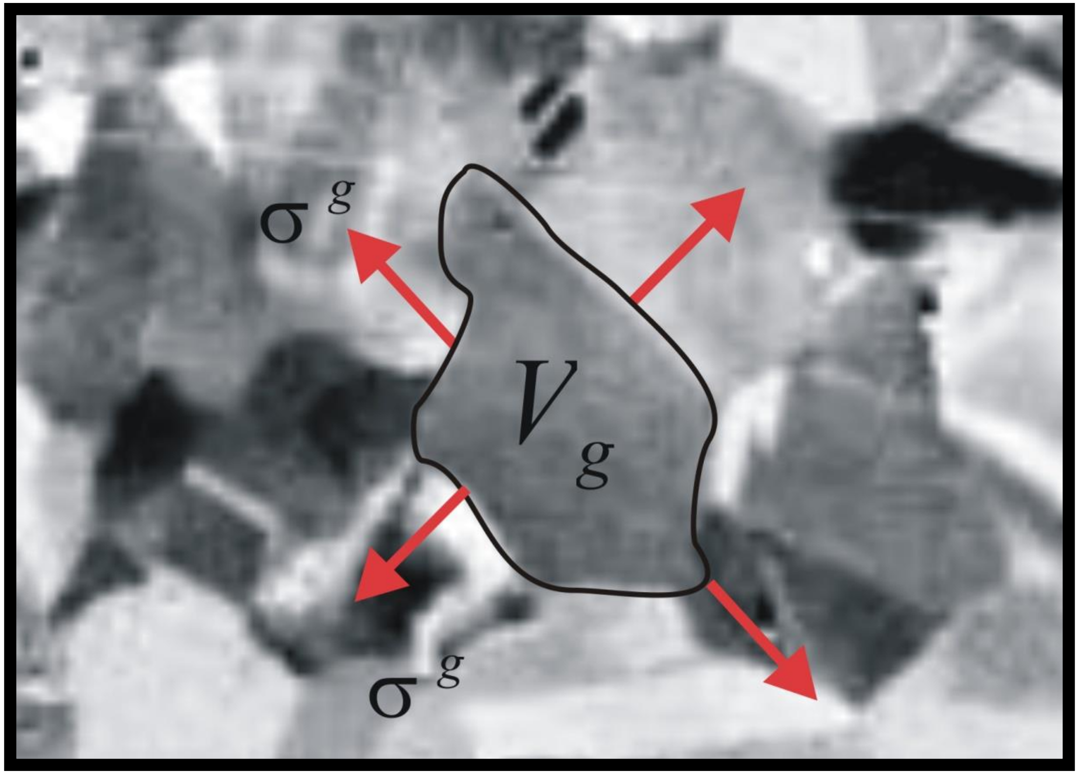

$$\sigma_{ij}^{IIg} = \sigma_{ij}^{g} - \sigma_{ij}^{I} \quad \text{where} \quad \sigma_{ij}^{I} = \sigma_{ij}^{M} \quad \text{for single phase material}$$

Effect of tensile elastic strain on Kikuchi band width

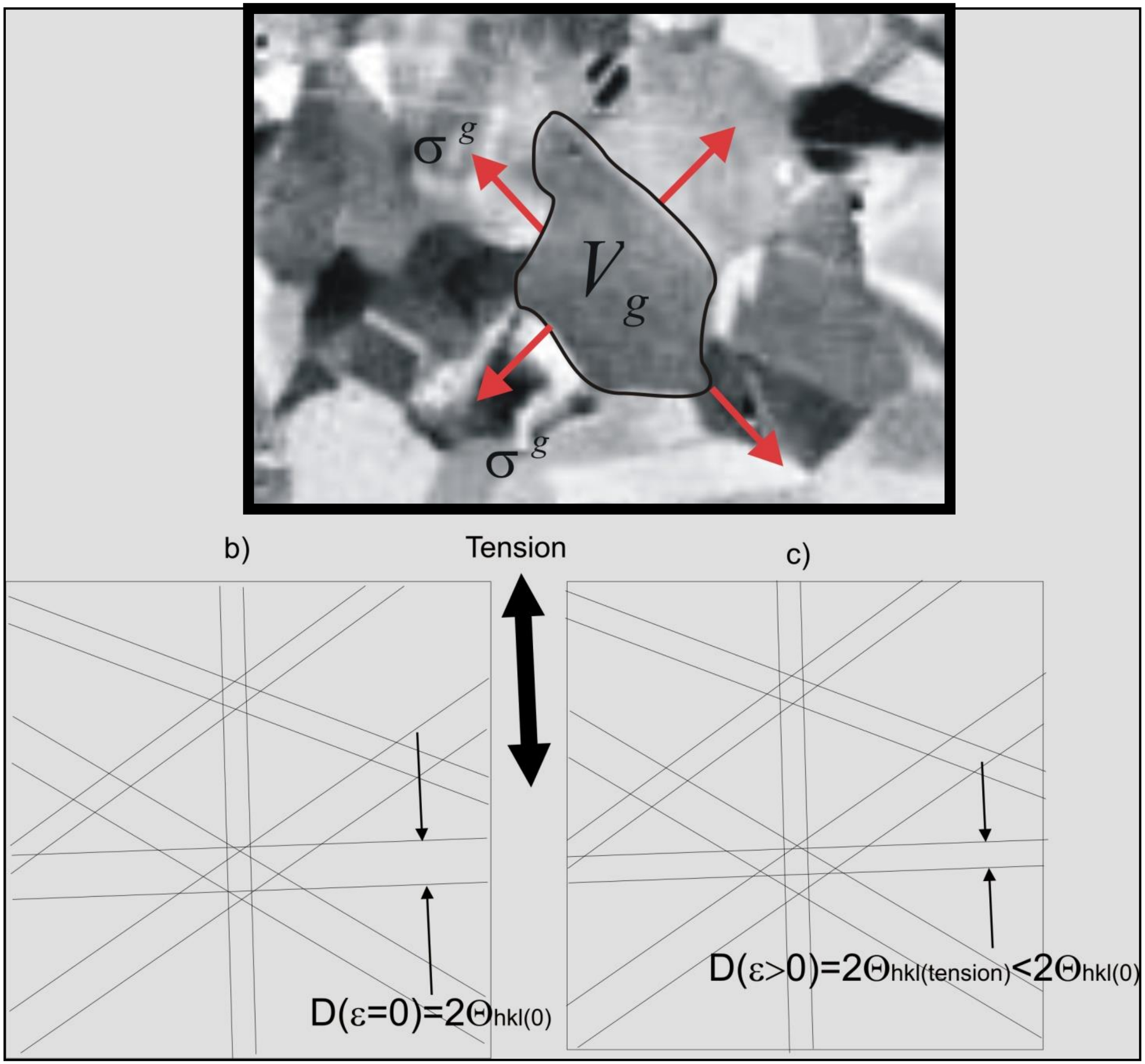

Second order stresses

Definition of different types of stresses at various spatial scales

Scale of the third order stresses

(the local stress at ***r*** position is indicated)

$$\sigma_{ij}^{III}(r) = \sigma_{ij}(r) - \sigma_{ij}^{g}$$

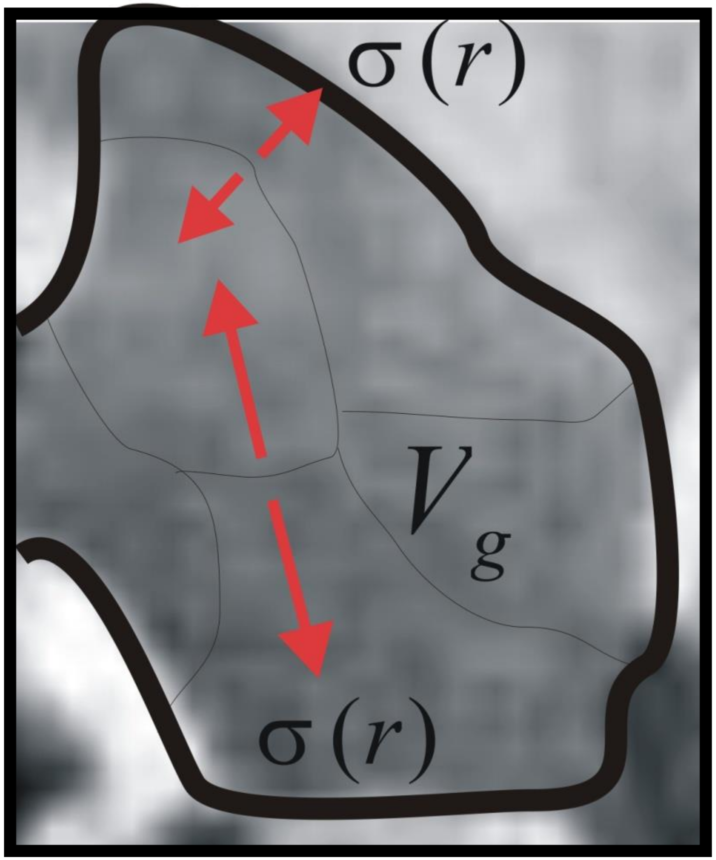

The broadening of original sharpness of diffraction line connected with the local strain (stress) associated with the local increasing of lattice defects concentration)

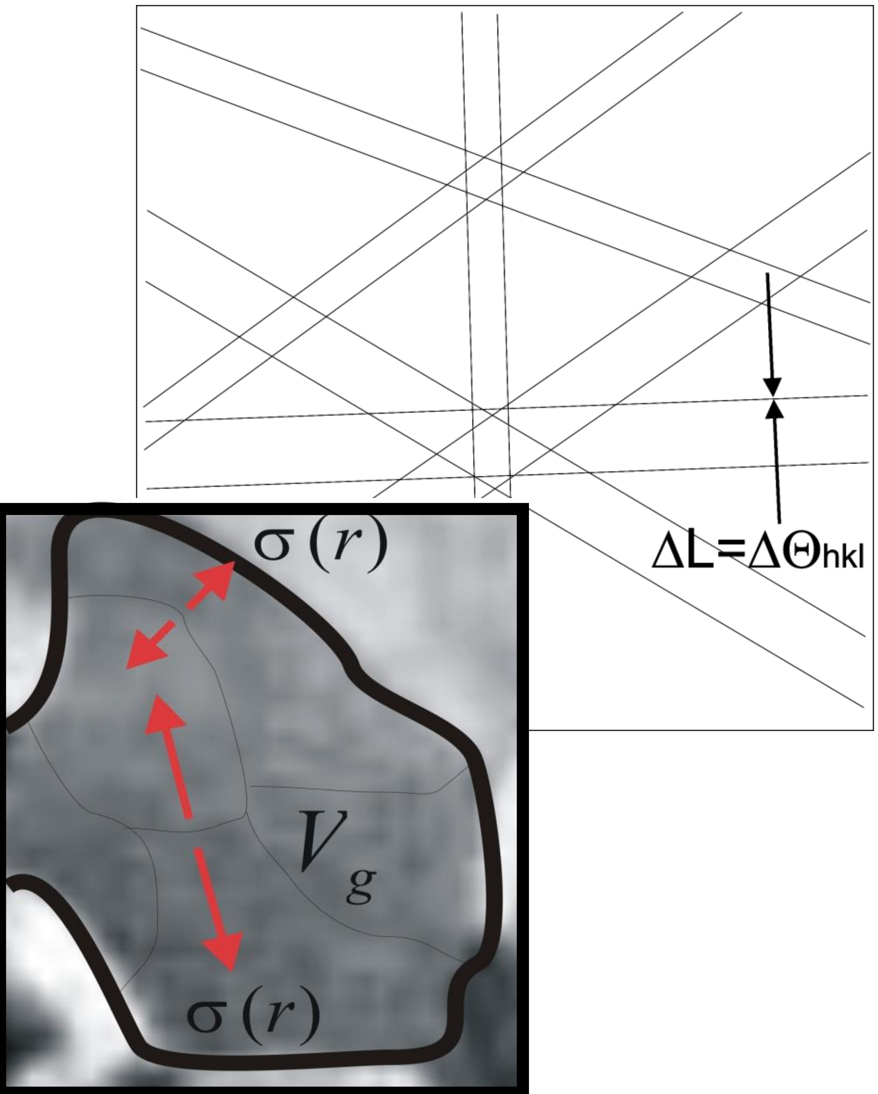

Third order stresses

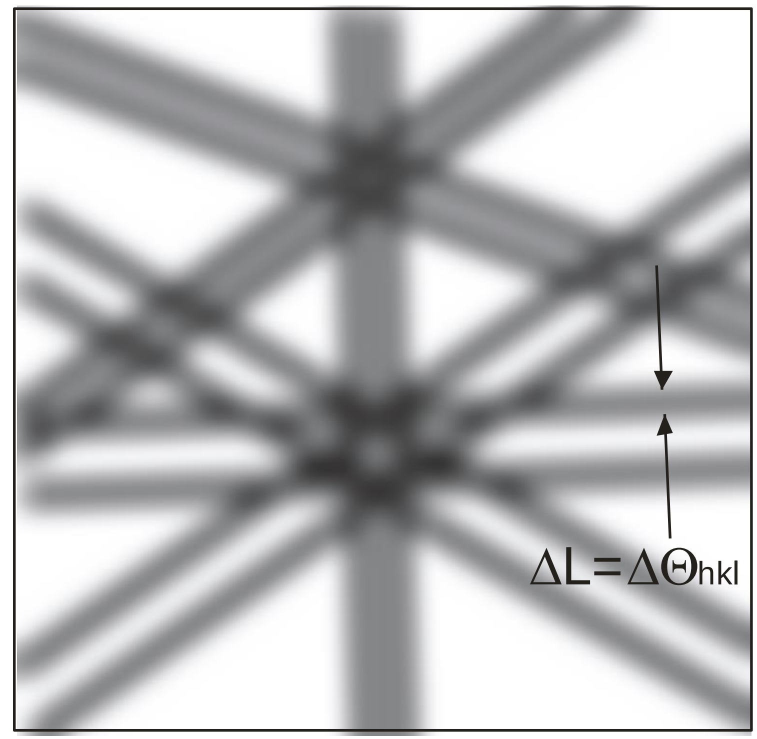

The originally sharp line edge associated with a single d-spacing broadens as numerous spacings contribute to the band.

The broadening of original sharpness of diffraction line connected with the local strain (stress) associated with the local increasing of lattice defects concentration)

Third order stresses

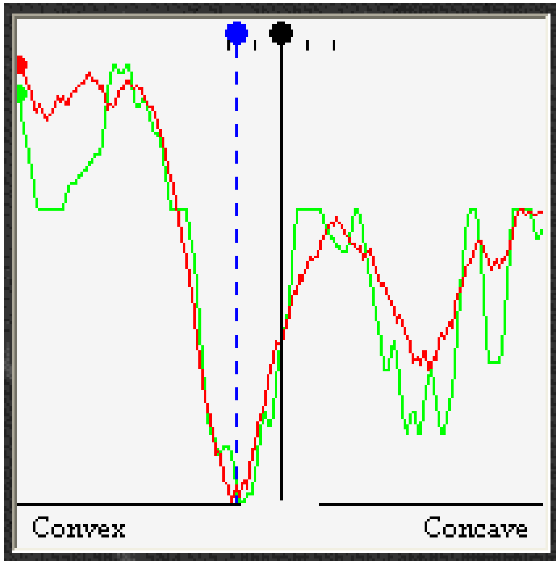

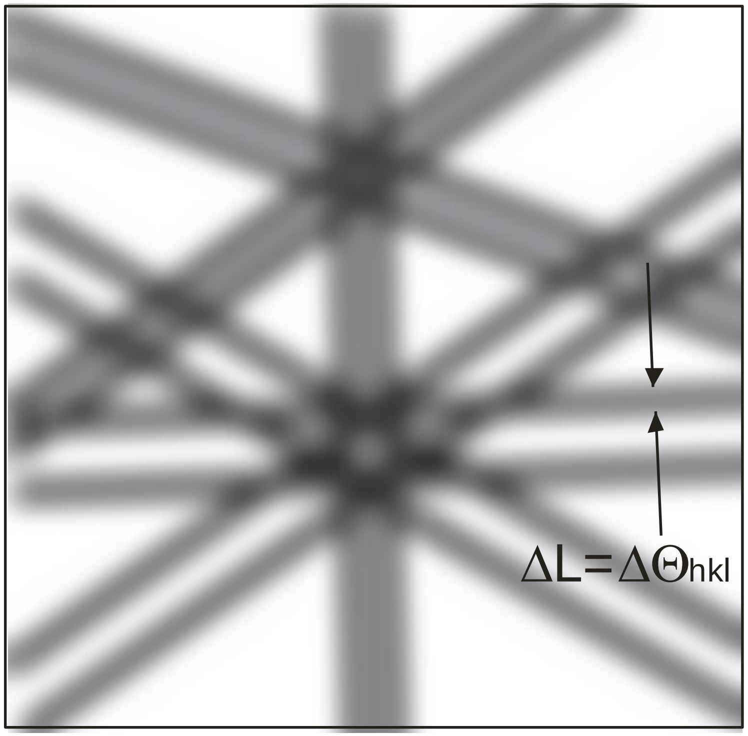

The originally sharp line edge associated with a single d-spacing broadens as numerous spacings contribute to the band.

EBSD measurements of surface local strains in alumina ceramic before shot peening (test sample).

coarse-grained ceramic

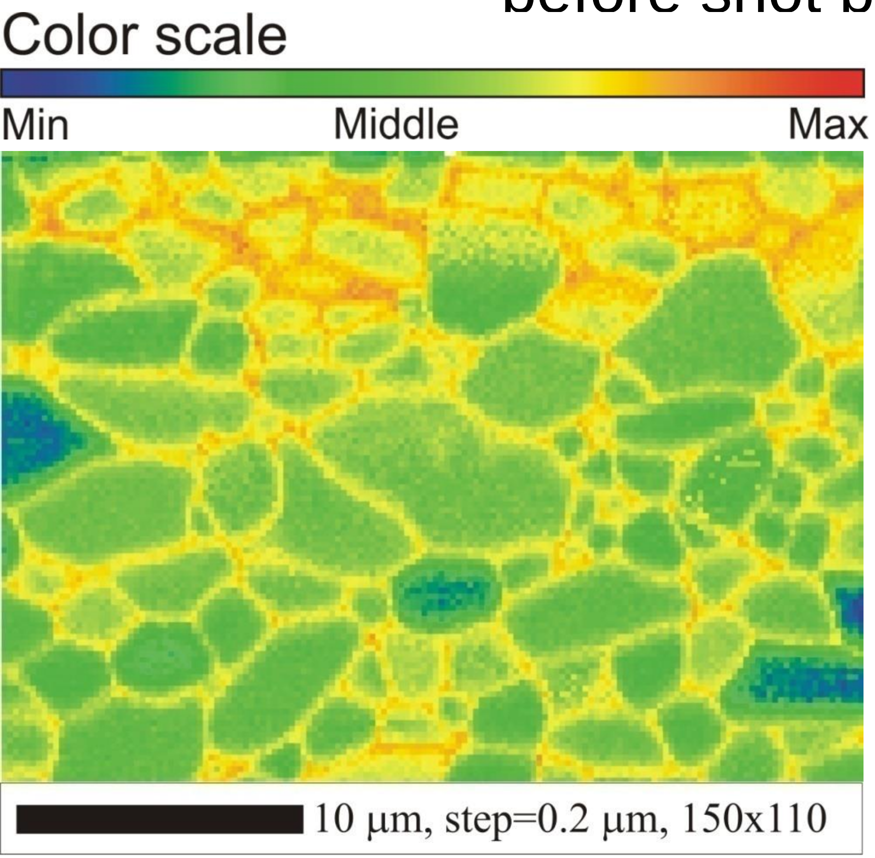

q map.

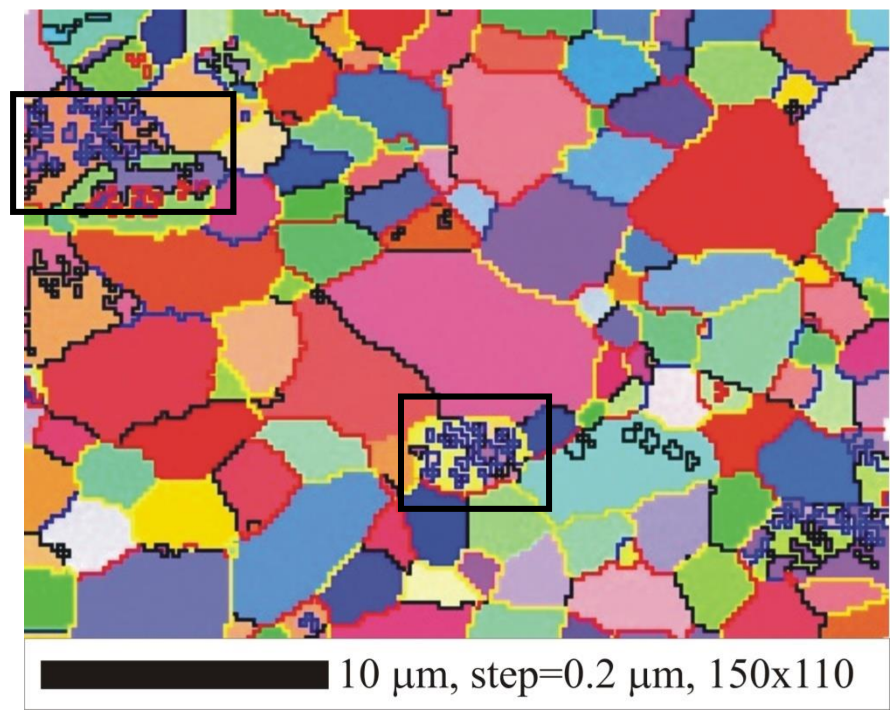

Orientation map; grain boundaries with disorientation angle 20 – 40º → blue, 40 – 60º → black, 60 – 80º → yellow, > 80º →

EBSD measurements of surface local strains in Al_2O_3 ceramic before shot peening

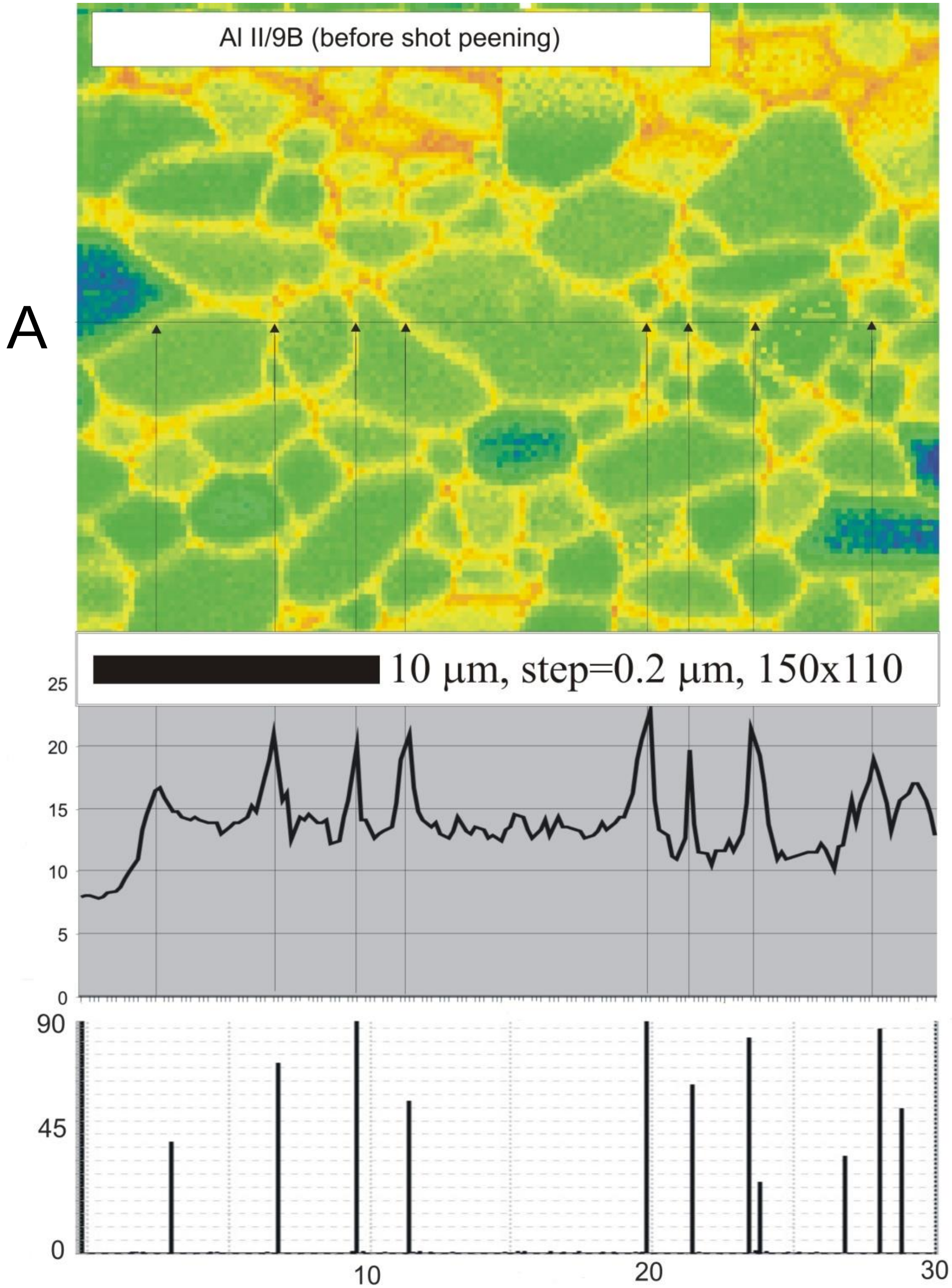

Map of Quality index (q)

Changes of Quality index (q) along the A-A line

Changes of misorientation angle along the A-A line

EBSD measurements of surface local strains in alumina ceramic after shot peening

fine-grained ceramic

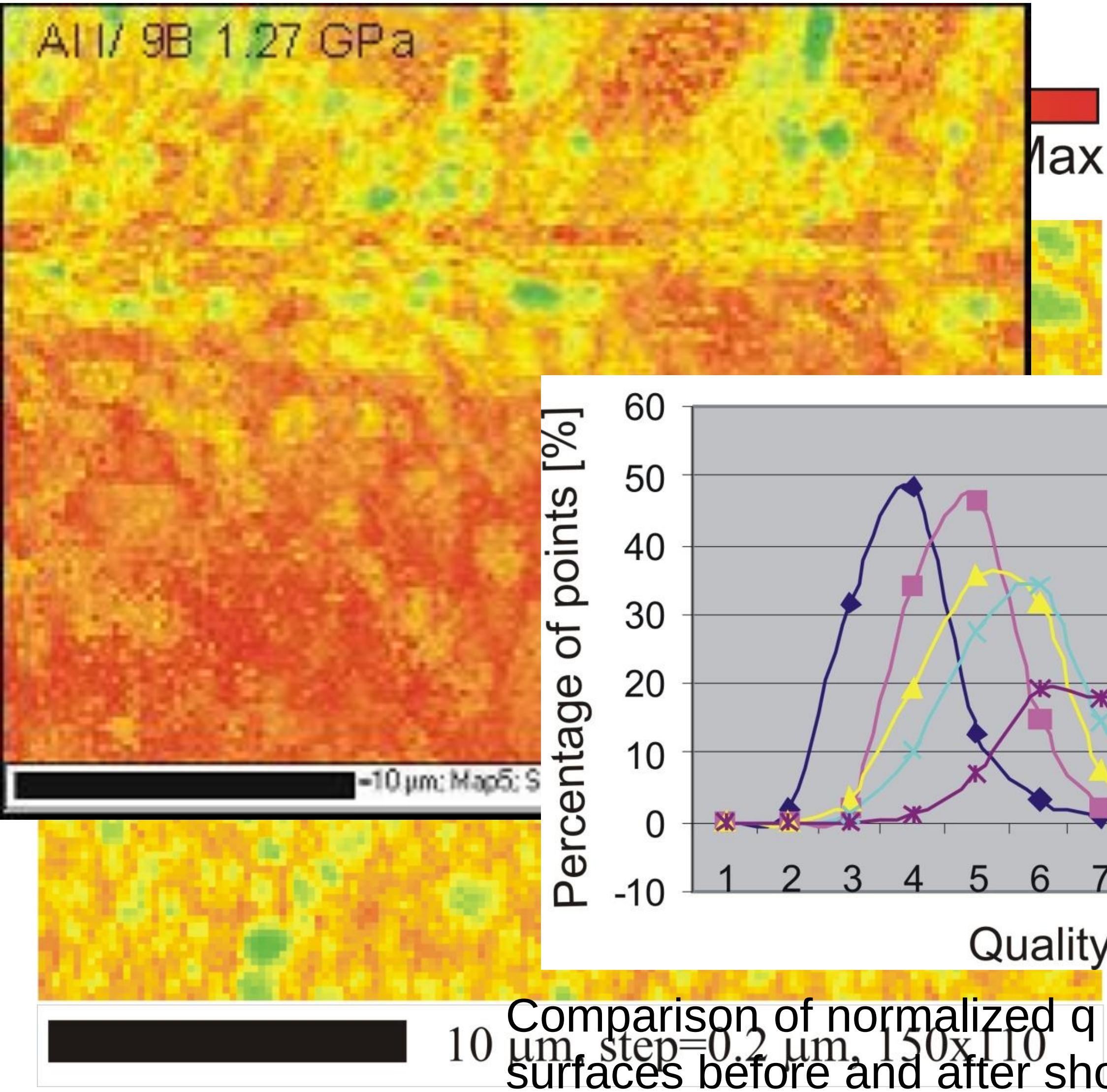

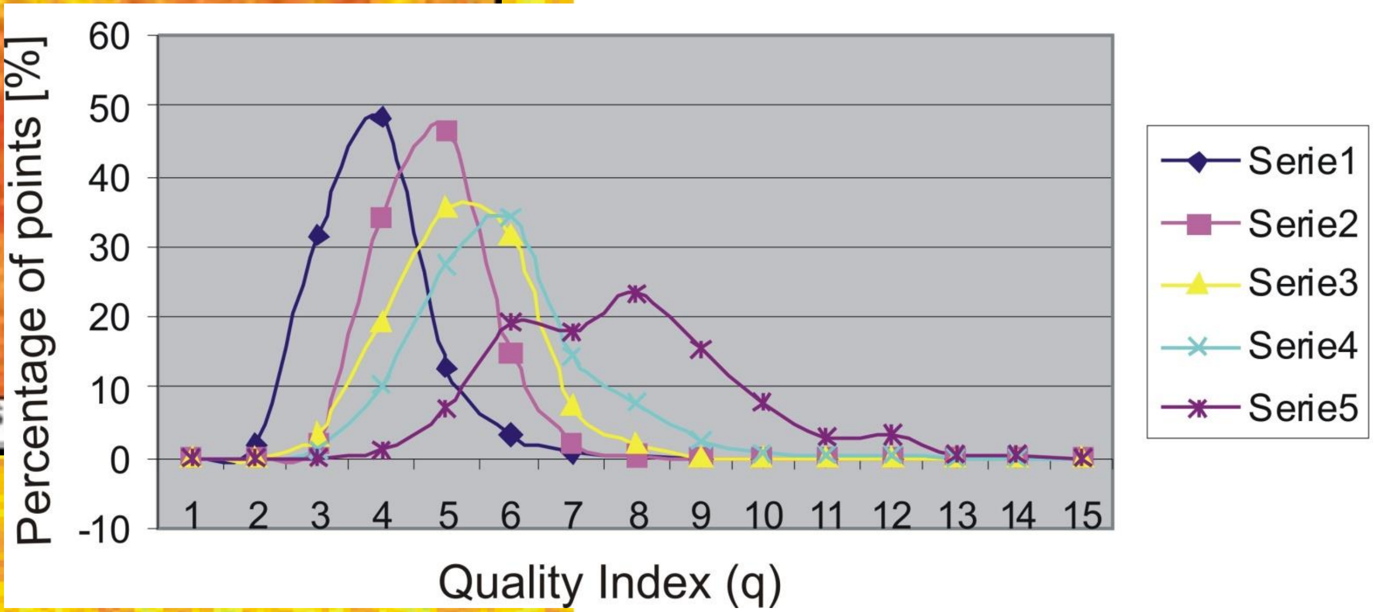

Comparison of normalized q distributions for alumina sample surfaces before and after shot peening: 1 – the test sample, 2 - (first order stresses ~0.35 GPa), 3 - (first order stresses ~0.083 GPa), 4 and 5 - (first order stresses 1.27 GPa).

EBSD measurements of local strains in copper after cold rolling, recrystallization and tension.

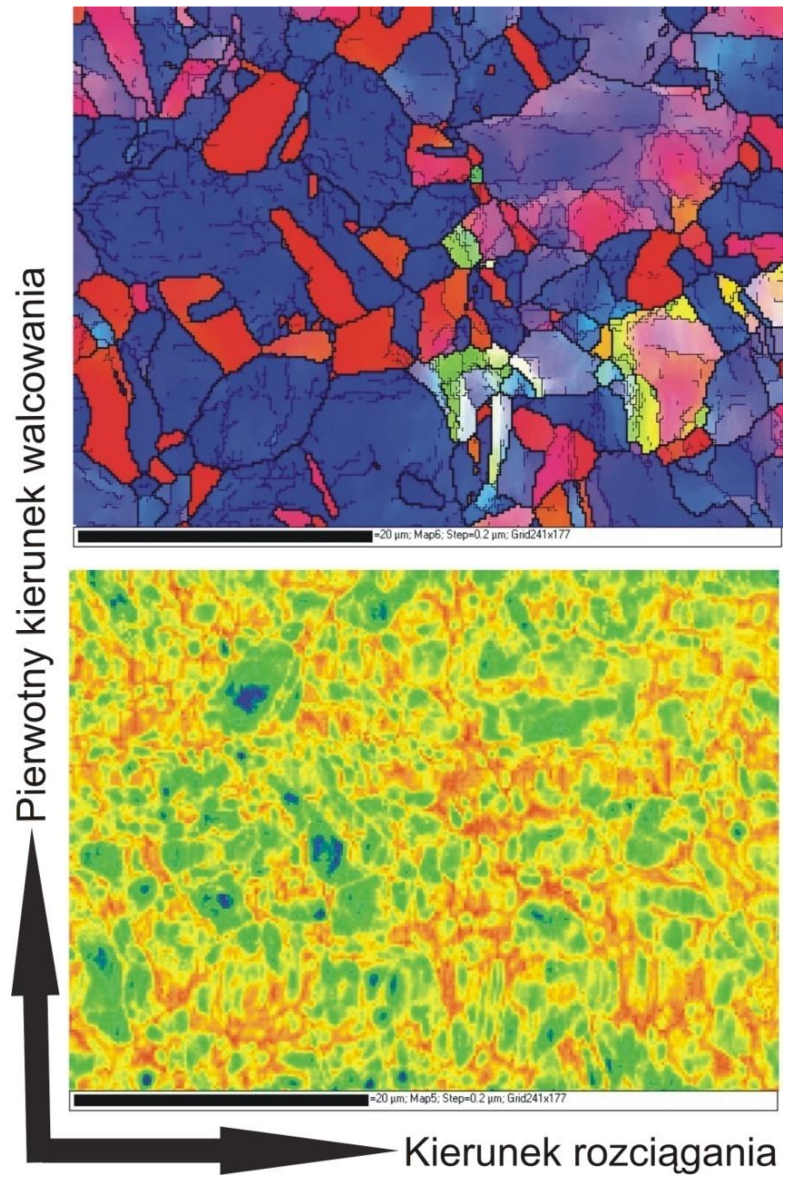

Conclusions

- **Microstructure refers to the assemblage of grains and other constituents such as pores and precipitates.**
- COM is a technique which allows crystal orientations to be measured.
- Maps of crystal orientation can be collected using SEM/COM and TEM/COM. <u>They remove any ambiguity regarding the recognition of grains and grain boundaries in the sample.</u>
- The grains in polycrystalline material are usually not randomly oriented, and crystallographic texturing can confer special properties on materials.
- COM is as an important technique for texture analysis because it allows the relation between texture and microstructure to be studied.
- Grain boundaries are the interfaces between grains. Boundaries formed between grains with particular orientation relationships to one another can have desirable properties.
- COM can characterise these boundaries and measure the distribution of various boundary types in a sample.
- **COM is a technique for microstructural analysis.**

Krzysztof Sztwiertnia

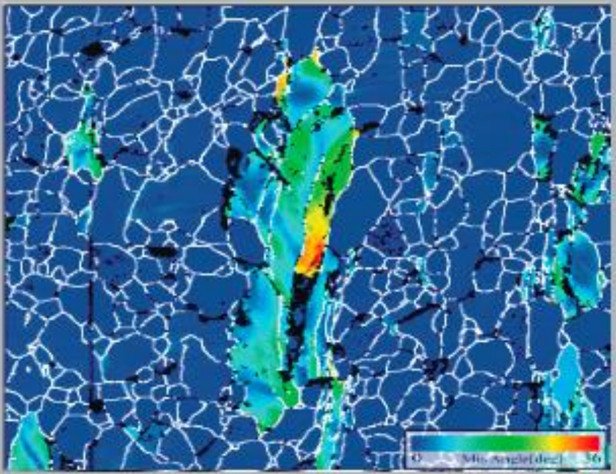

Orientacja krystalograficzna w badaniach mikrostruktury materiałów

Polska Akademia Nauk
Instytut Metalurgii I Inżynierii Materiałowej
Kraków 2009